HELICOPTER CRASHWORTHINESS RESEARCH PROGRAM

Gary L. Farley and Richard L. Boitnott

Aerostructures Directorate
USAARTA-AVSCOM
National Aeronautics and Space Administration
Langley Research Center

and

Huey D. Carden

National Aeronautics and Space Administration
Langley Research Center

Results are presented from the U.S. Army-Aerostructures Directorate/NASA-Langley Research Center joint research program on helicopter crashworthiness. Through the on-going research program an in-depth understanding has been developed on the cause/effect relationships between material and architectural variables and the energy-absorption capability of composite material and structure. Composite materials were found to be efficient energy absorbers. Graphite/epoxy subfloor structures were more efficient energy absorbers than comparable structures fabricated from Kevlar or aluminum. An accurate method of predicting the energy-absorption capability of beams was developed.

INTRODUCTION

The design requirements in Mil-Std-1290, reference 1, define the crash scenarios that must be survivable for the occupants of U.S. Army helicopters. Vehicle crashworthiness, as specified in Mil-Std-1290, requires the maintainance of a protective shell around the occupants in addition to absorbing vehicle kinetic energy. In the case of a helicopter the protective shell is the fuselage structure. The crash induced loads in the helicopter fuselage structure, per the requirements of Mil-Std-1290, are generally greater than loads from other flight or ground conditions.

In the next generation of military helicopters, composite materials will be used extensively in all primary structure. Composite materials offer considerable potential advantages over metallic materials from the perspective of weight and fabrication cost. However, composite materials and structures exhibit brittle failure characteristics, in contrast to the benign ductile failure characteristics of most metallic structures.

Prior to the design of the next generation of military helicopters, sufficient technology must be developed to design crashworthy fuselage structure utilizing composite materials. This technology includes understanding the cause/effect relationships of energy absorption in composite materials and developing analysis tools and design methodology. Once the material response is understood, efficient energy absorbing structural subfloor concepts can be developed.

The U.S. Army Aerostructures Directorate and NASA's Langley Research Center formed a joint research program to develop the technology required to design crashworthy composite helicopter structure. This program consists of a material characterization phase, a structural element phase, and a fuselage section demonstration phase. The material characterization phase consists of investigations to understand how composite materials absorb energy and how the numerous material and architectural variables effect energy-absorption capability. The structural element phase consists of two parts: subfloor structure and fuselage structural integrity. Investigations conducted in the structural element phase include the development of energy absorbing subfloor beam concepts, analysis methods, and fuselage structural integrity. The final phase, a fuselage section demonstration, includes the design and fabrication, of representative floor and fuselage sections. These sections will be tested using static load and dynamic impact conditions.

This paper presents the results obtained to date in the material characterization and structural element phases. Recent developments in energy absorbing composite materials and structures are described. Finally, results are presented from composite fuselage frame investigations.

SYMBOLS

A	cross sectional area, cm^2.
D	internal diameter of circular cross section tubes, cm.
E	epoxy matrix.
F	woven fabric material.
Gl	glass fiber reinforcement.
Gr	graphite fiber reinforcement.
H	graphite/Kevlar hybrid 24 by 24 balanced woven fabric material.
$i_{C.E.}$	i^{th} characteristic element.
K	Kevlar fiber reinforcement.
N	number of plies.
n	number of characteristic elements.
S	symmetric ply layup.
S.E.	structural element.
T	tape material.
t	tube wall thickness, cm.
W	internal width of square cross section tubes, cm.
D/t	diameter-to-thickness ratio of circular cross section tubes.
W/t	width-to-thickness ratio of square cross section tubes.
σ	average crushing stress, Pa.
ρ	material density, gr/cm^3.
θ	ply orientation angle.
σ/ρ	specific sustained crushing stress, Nm/gr.

TERMINOLOGY

Specific sustained crushing stress - average crushing load divided by the product of the specimen cross sectional area and the material density.

Characteristic crushing length - the nominal length of the crushed material.

Bias ply - composite ply oriented at any direction other than along the longitudinal or transverse axis of the specimen.

DYCAST - finite element computer code, Dynamic Crash Analysis of Structures, reference 2.

ENERGY ABSORPTION CHARACTERISTICS OF COMPOSITE MATERIAL

Design of efficient energy absorbing structure requires understanding the cause/effect relationship between the material and architectural variables and the energy-absorption capability of composite materials. Composite materials and structures absorb energy in modes that are considerably different than those of metallic materials and structures. Tailoring the mechanical response of composites using material property variables (fiber and matrix stiffness and failure strain) and architectural variables (ply orientation, stacking sequence, hybridization, fiber volume fraction, and specimen geometry) is well understood. However, the manner in which these variables affect the energy-absorption capability of composite materials is not well understood. Studies were conducted to further define the energy absorption process of composite materials. These studies included definition of the crushing process and crushing modes and the energy absorption efficiency of several composite materials and an investigation of what effect material property variables, architectural variables, and crushing speed have on the energy-absorption capability of composite materials.

In the following discussion, data are presented in terms of the specific sustained crushing stress (σ/ρ). Specific sustained crushing stress is a measure of energy-absorption capability.

Crushing Modes/Processes

Four different crushing modes and combinations of the four modes have been identified for composite materials, as reported in references 3-8 and depicted in figure 1. These four modes are 1) local buckling, 2) transverse shearing, 3) brittle fracturing, and 4) lamina bending. The local buckling mode is similar to that exhibited by ductile metals. This crushing mode has been demonstrated by both ductile (Kevlar) and brittle (graphite and glass) fiber reinforced composites. Ductile fiber composites always exhibit the local buckling crushing mode. Ductile fibers plastically deform at the buckle site along the compression side of the buckled fibers. The fibers can also split into small fibrils along the tension side of the buckled fibers. Ductile fiber reinforced composites remain intact after being crushed and thereby demonstrating post-crushing integrity. The post-crushing integrity of ductile fiber reinforced composites is a result of fiber plasticity and fiber splitting. Brittle fiber composites only exhibit the local buckling crushing mode when the ply orientations are such that interlaminar stresses which are small relative to the strength of the matrix and when the matrix is a high failure strain and low stiffness material. The combination of a high failure strain/low stiffness matrix with certain ply orientations reduces or prevents interlaminar cracking from occurring in the crushing process. If the interlaminar cracks are eliminated the, tube crushes in the local buckling mode or fails catastrophically and is unable to carry load.

The brittle fracturing, lamina bending, and transverse shearing modes are exhibited exclusively by brittle fiber reinforced composites. These crushing modes are a function of the mechanical properties of the constituent materials. Generally, one or multiple interlaminar cracks are formed through the thickness of the composite. The number, location, and length of the cracks are a function of architecture and constituent material properties. The interlaminar cracks form lamina bundles which can act as columns. As the load is applied the interlaminar cracks grow until the column buckles and either the edges of the column are sheared away forming a conical shaped cross section (transverse shearing mode), fractured (brittle fracturing mode), or bent (lamina bending mode).

Just as strain rate can effect the mechanical response of a material, crushing speed can effect the energy-absorption capability of composite materials. To understand how crushing speed influences energy-absorption capability it is necessary to determine how crushing speed affects the mechanisms that control the crushing process.

The controlling mechanisms in the four crushing modes are: transverse laminate strength (transverse shearing crushing mode), matrix strength (brittle fracturing and lamina bending crushing modes), lamina bundle bending strength (brittle bracturing crushing mode), and fiber/matrix yield strength (local buckling crushing mode). The transverse strength of a laminates typically used in helicopter structural applications is primarily a function of fiber strength. Therefore, if the fiber's mechanical response is a function of strain rate then the energy-absorption capability of specimens that crush in a transverse shearing mode can be a function of crushing speed.

Matrix strength controls the interlaminar crack growth in both the brittle fracturing and lamina bending crushing modes. Many polymeric matrix materials exhibit mechanical responses that are a function of strain rate. Therefore, a specimen that exhibits either the brittle fracturing mode or lamina bending mode can exhibit energy-absorption capability that is a function of crushing speed. Crushing speed will effect energy-absorption capability when the percentage of energy absorbed by the interlaminar crack growth is a significant part of the total energy absorbed. For that reason, specimens that crush in the lamina bending mode will be more affected than specimens that crush in the brittle fracturing mode. In the lamina bending crushing mode a significant portion of the total energy absorbed is by interlaminar crack growth, whereas the converse is true for the brittle fracturing mode.

The bending strength of the lamina bundle controls the fracturing of the lamina bundle in the brittle fracturing crushing mode. The mechanical response of the lamina bundle is primarily a function of either fiber (e.g., 0 degree lamina bundle) or matrix (e.g., 90 degree lamina bundle or low fiber volume fraction material). Therefore, if the mechanical response of the dominant property (fiber or matrix) is a function of strain rate then the energy-absorption capability of the lamina bundle can be a function of crushing speed.

The mechanism that controls the local buckling crushing mode is the yield strength of the fiber and/or matrix. Brittle fiber reinforced composites can produce the local buckling crushing mode only if the matrix has a low stiffness and high failure strain. If the matrix mechanical response is a function of strain rate then the energy-absorption capability can be a func-

tion of crushing speed. Ductile fiber reinforced composites crush in the local buckling mode because of either the fiber or matrix properties. Therefore, if either the fiber or matrix mechanical response is a function of strain rate then the energy-absorption capability can be a function of crushing speed.

ENERGY-ABSORPTION EFFICIENCY

Debris size of crushed material (characteristic crushing length) is a qualitative measure of energy-absorption efficiency. The characteristic crushing length of specimens that exhibit transverse shearing mode, brittle fracturing mode, lamina bending mode, and local buckling mode are on the order of a lamina thickness, a laminate thickness, 10-100 laminate thicknesses, and 10-50 laminate thicknesses, respectively. The smaller the characteristic crushing length the greater the energy-absorption efficiency. This ordering of energy-absorption crushing efficiency is applicable only to specimens of the same material. Different materials have different energy-absorption potential. A specimen fabricated from a material that has a high energy-absorption potential can have a greater energy-absorption capability despite a less efficient crushing mode than a specimen fabricated from a material that has a lower energy-absorption potential but crushes in a more efficient mode.

EFFECT OF MATERIAL PROPERTIES

Fiber and Matrix Failure Strain

A series of studies, references 9 and 10, were performed to determine the effect of fiber and matrix failure strain on energy-absorption capability of graphite and Kevlar reinforced composites. These studies were conducted using low failure strain (T300), intermediate failure strain (AS4) and high failure strain (AS6) graphite, and with Kevlar fibers. These fibers were embedded into low failure strain (934), intermediate failure strain (5245 and 974), high failure strain (F185), and toughened interleafed (HST-7) matrices. Table 1 presents the combinations of these fibers and matrices used in this study. Based upon the results of these studies, as shown in figures 2 and 3, composite materials composed of low and intermediate failure strain graphite fibers and matrices (T300/934, AS4/934, T300/5245, and AS4/5245) generally exhibit an increase in energy-absorption capability as failure strain increased. The predominant crushing mode of the materials was a brittle fracturing mode with lamina bending. The energy-absorption trends for the low and intermediate failure strain material are generally consistent with mechanical response trends of these composites. However, these trends do not hold for high strain fiber and matrix material (AS6/F185) and the high strain fibers in a toughened matrix material (AS6/HST-7) as shown in figure 4. The crushing mode of the high strain material changed from a predominantly brittle fracturing to a predominantly lamina bending mode or to a local buckling crushing mode. The energy-absorption capability of the high strain and toughened composites were substantially less than the intermediate strain (AS4/5245) material. The crushing mode of the toughened material was a mixture of brittle fracturing and lamina bending and energy-absorption capability was similar to that exhibited by the AS4/934 material. The toughened interleafed material consists of a low failure strain matrix, similar to the 934 matrix, with a high failure strain adhesive between the plies. The adhesive

layer was ineffective in stopping the interlaminar cracks because the cracks formed in the low failure strain matrix adjacent to the adhesive layer.

Similar studies were conducted using Kevlar-49 in 934 and 974 matrices to determine the effect of matrix failure strain on the energy-absorption capability of a ductile fiber reinforced composite material. As shown in figure 5, a 5 to 15 percent decrease in energy-absorption capability occurred as matrix failure strain increased from 1 to 2 percent. The crushing mode and crushing load level are primarily controlled by the compression characteristics of the fiber. Kevlar fibers exhibit an inherent failure mechanism related to its plastic deformation. Therefore, matrix failure strain would have little effect on altering the fiber failure load or mode.

Effect of Fiber Stiffness

The effects of fiber stiffness, reference 10, on the energy-absorption capability were evaluated for brittle fiber reinforcements using T300, P55, and P75 graphite fibers in a common matrix (934). It is difficult in studies of this type to isolate the effects of a single property on energy-absorption capability. Two cases were cited in the previous section where a change in a secondary material property altered the crushing response. In this evaluation the effects of fiber stiffness were studied. However, the fibers have significantly different failure strains. The failure strain of the T300, P55, and P75 graphite fibers are 0.012, 0.005, and 0.004, respectively.

Figures 6 and 7 show that energy-absorption capability decreased nonlinearly with respect to increasing fiber stiffness. The difference in energy-absorption capabilities demonstrated by the material systems is proportional to the difference in fiber failure strain. This proportionality between energy absorption and fiber failure strain is apparent upon examining the energy-absorption trends for ply orientations where fibers are principally oriented in the direction of the applied load such as $[0/\pm15]_4$ and $[\pm15]_6$. These results suggest that changes in fiber stiffness affect energy-absorption capability less than changes in fiber failure strain, provided the different materials crush in the same mode. The P55/934 and P75/934 material exhibited a progressive transverse shearing crushing mode. The residue formed by crushing the P55/934 and P75/934 was like powder whereas residue from the T300/934 material was coarser. These results indicate that the high failure strain brittle fibers, such as glass, have significant potential for absorbing energy provided the load carrying fibers can be sufficiently stabilized to crush in a transverse shearing or a brittle fracturing mode.

EFFECT OF SPECIMEN ARCHITECTURE

Effects of Ply Orientation and Material Form

Ply orientation is one of the most important variables available to the composite structural designer to tailor the mechanical response of a composite laminate. The stiffness and strength of a laminate are a direct function of the ply orientation. However, energy-absorption capability is not as well defined. The effects of ply orientation on the crushing response of tube specimens was investigated.

Tests were conducted, reference 3, on T300/934 (Gr/E), E-Gl/934 (Gl/E), and K/934 (K/E) tube specimens, as shown in figure 8, to determine the effect of ply orientation on energy-absorption capability. Only the results from the $[0/\pm\theta]_4$ specimens will be discussed. The energy-absorption trends for the materials differed significantly. As the ply angle increased, the energy-absorption capability of the Gr/E material decreased. This trend is consistent with the general mechanical response of such composites. However, the opposite trend occurred for the Gl/E and K/E material. Energy-absorption capability generally increased with increasing ply angle. The difference in energy-absorption trends can be explained by examination of the crushing modes.

The Gr/E specimens crushed in a brittle fracturing mode while the Gl/E and K/E specimens crushed in a lamina bending and local buckling mode, respectively. As previously discussed, the brittle fracturing mode exhibited by the Gr/E is a more efficient energy-absorption mode than the lamina bending or the local buckling modes. These energy-absorption trends can be related to the constituent properties of the fiber and matrix.

In the case of the Gr/E specimens, the matrix is sufficiently stiff and has sufficient failure strain to stabilize the axially oriented Gr fibers. Therefore, the crushing load, hence energy-absorption capability, is a function of axial stiffness. At bias ply orientations greater than 45 degrees, the bias plies began to provide lateral support to the axially oriented fibers. That is, the bias plies helped the matrix. Beyond 60 degrees the loss of axial stiffness balanced out the increased lateral support provided by the bias plies and resulted in a relatively constant energy-absorption capability.

The glass fibers in tube specimens that have fibers oriented in the direction of the applied load are not adequately stabilized by the matrix which results in a less efficient energy-absorption mode (lamina bending). As the bias plies become more circumferentially oriented the energy-absorption capability increased even though the axial stiffness decreased. At bias ply angles greater than 45 degrees, the bias plies provide lateral support to stabilize the axial fibers. Further increase in circumferential fiber angle beyond 60 degrees provided no additional support to the axial fibers. A similar crushing scenario applies to the K/E specimens except that the K/E specimens crushed in a local buckling mode.

Another important parameter influencing energy-absorption capability is the material form, such as tape, planar woven, or filament wound material. The majority of the studies have been performed with specimens fabricated using tape and planar woven composite prepreg material. The characteristic crushing length of the tape material is a function of the fiber and matrix mechanical properties and ply orientation as previously discussed. The woven material has a built-in failure initiator at each undulation of the reinforcement tow. These undulations can predetermine the characteristic crushing length of the material. In the case of glass reinforced composites, the undulations of the woven material can change the crushing modes from lamina bending to a brittle fracturing mode. Changes of this type can influence the energy-absorption capability. If the characteristic crushing length of a specimen is less than the spacing of undulations, then the woven material will have a lower energy-absorption capability than the nonwoven material. In this case, the undulation reduces the bending stiffness of the lamina bundles resulting in a lower

energy-absorption capability for the woven material. Filament wound specimens typically crush in modes similar to those of specimens fabricated using tape prepreg provided the interleave spacing is greater than the characteristic crushing length.

Effects of Stacking Sequence

Lamina stacking sequence can be an important variable in tailoring the bending stiffness of a composite laminate and, therefore, will have significant implications with respect to energy-absorption capability, as reported in reference 10. Figure 9 shows the effect of stacking sequence on a hybrid composite and figure 10 examines this same effect on Gr/E and K/E [±45] composites.

Figure 9 shows the effect of stacking sequence on the energy-absorption capability of $[+45^{H}_{F}/0^{Gr}_{10T}/-45^{H}_{F}]$ and $[0^{Gr}_{5T}/\pm45^{H}_{F}/0^{Gr}_{5T}]$ tube specimens. The difference between these two stacking sequences is the position of the 0 degree Gr/E plies. In the first specimen the 0 degree Gr/E plies are in the center of the layup, whereas, the 0 degree Gr/E plies are on the outside in the second specimen. A 300 percent difference in energy-absorption capability was obtained for these hybrid composite specimens. The difference in energy-absorption capability is attri-buted to the crushing mode of the 0 degree plies. The 0 degree graphite plies of the $[+45^{H}_{F}/0^{Gr}_{10T}/-45^{H}_{F}]$ specimens crushed in a brittle fracturing mode while the 0 degree graphite plies of the $[0^{Gr}_{5T}/\pm45^{H}_{F}/0^{Gr}_{5T}]$ specimens crushed in a lamina bending mode. Both types of specimens exhibited post-crushing integrity as a result of the hybrid woven fabric plies. Current composite design practice would avoid layups concentrating all the 0 degree plies either in the center or on the outer surfaces. From an energy absorption consideration the 0 degree plies should not be located on the outer surfaces.

Stacking sequence does not always have as significant effect on energy-absorption capability. In figure 10 the test results of two different combinations of [±45] Gr/E plies and three different combinations of [±45] K/E plies are presented. Only a 5 percent change in energy-absorption capability was demonstrated by the $[\pm45]_6$ and $[\pm45_3/\mp45_3]$ Gr/E specimens. Both $[\mp45]_6$ and $[\pm45_3/\mp45_3]$ Gr/E specimens exhibited the characteristic brittle fracturing mode. The energy-absorption capability of the $[+45_6/-45_6]$ K/E specimens was approximately 30 percent lower than the $[\pm45]_6$ and $[\pm45_3/+45_3]$ K/E specimens. The $[+45_6/-45_6]$ specimens exhibited the characteristic buckling crushing mode although more extensive interlaminar delaminations occurred than in the $[\pm45]_6$ or $[\pm45_3/\mp45_3]$ specimens. Conventional manufacturing practices typically do not allow the segregation of plies in a manner representative of the $[+45_6/-45_6]$ layup. Therefore, for most practical combinations of 45 degree plies stacking sequence has negligible effect on energy absorption.

A third example will demonstrate how concentrating all the plies in the center of the laminate can lead to unexpected results. A series of tests were conducted on $[\pm45^{K}/0^{Gr}_{N}]_S$ ply orientations where N=3, 6, 9, and 12. The test results are shown in figure 11 and typical crushed tubes are shown in figure 12. In this study, the ply orientations of the K/E plies were at ±45 degrees which is representative of typical ply orientations in helicopter subfloor beams. The unidirectional Gr/E plies were oriented such that the fibers were in the direction of the applied crushing load, i.e., in the direction to achieve maximum energy-absorption capability.

Previous tests had shown that increasing the percentage of graphite plies oriented in the direction of applied load would produce higher energy-absorption capability. The test results shown in figure 11 exhibit the opposite trend. The reason for this trend is evident upon examination of the crushing modes shown in figure 12. As N (the number of 0 degree plies) increased, the crushing mode of the Gr/E plies changed from a brittle fracturing mode, to a predominantly lamina bending mode. However, in all cases the energy-absorption capability of $[\pm 45^{K}/0^{Gr}{}_{N}]_{S}$ exceeds the energy-absorption capability of aluminum. Ideally the circumferentially oriented plies (i.e., the K/E plies) should be interspersed through the laminate which would insure the Gr/E plies crush in a brittle fracturing mode.

Effect of Fiber Volume Fraction

The effect of fiber volume fraction, reference 10, on the energy-absorption characteristics of Gr/E and K/E composites is shown in figures 13 and 14, respectively. Prepreg materials with different percentages, between 40 and 70 percent, of fiber (by volume) were used to make tube specimens. As shown in figure 13, the $[\pm 45]_6$ and $[0/\pm 15]_4$ specimens exhibited an approximate 10 percent decrease in energy-absorption capability while the $[0/\pm 75]_4$ specimens exhibited an insignificant change in energy-absorption capability as fiber volume fraction increased between 40 and 55 percent. As the volume of matrix between fibers decreases, the interlaminar strength of the composite typically decreases. As the interlaminar strength decreases, interlaminar cracks form at lower loads, resulting in a reduction in energy-absorption capability. Also, as fiber volume fraction increases the density of the composite increases which results in a lower energy-absorption capability.

The effect of fiber volume fraction on energy-absorption capability of Kevlar reinforced composites is shown in figure 14. Between fiber volume fractions of 46 and 55 percent, the change in energy absorption was negligible for all ply orientations. The densities of the Kevlar fiber and the matrix are similar, therefore fiber volume fraction has little effect on energy-absorption capability provided the reduction in matrix between fibers does not affect the crushing mode. Both the $[\pm 45]_6$ and $[0/\pm 75]_4$ ply orientations exhibited approximately a 10 percent decrease in energy-absorption capability between fiber volume fractions of 54 and 70 percent. The energy-absorption capability of the $[0/\pm 15]_4$ ply orientation increased approximately 10 percent between fiber volume fractions of 55 and 66 percent.

Effects of Material Hybridization

The term hybrid composite material encompasses a large class of composite materials. Hybrids include both combinations of different reinforcement fibers in a laminate or a combinations of different material forms of the same fiber system such as tape and fabric. Most of the specimens that were fabricated with hybrid materials had different reinforcement fibers such as graphite-Kevlar or graphite-glass. Kevlar exhibits a local buckling crushing mode and has post-crushing integrity, which may be advantageous for certain structural applications. However, Kevlar composites are not as efficient energy absorbers as graphite composites. There are applications, such as the subfloor structure, where combining the post-crushing integrity characteristics of Kevlar with the high energy-absorption capability of graphite can

be beneficial.

A number of studies, references 3 and 10, have been conducted to evaluate the energy-absorption potential of hybrid materials. Only two of these materials will be discussed here. Figure 15 depicts the energy-absorption capability of $[\pm 45^{H}_{F}]_2$ Gr-K/E and $[+45^{H}_{F}/0^{Gr}_{5T}]_S$ materials. The $[\pm 45^{H}_{F}]_2$ hybrid woven fabric material is a balance weave fabric composed of alternating tows of graphite and Kevlar reinforcement. The $[+45^{H}_{F}/0^{Gr}_{5T}]_S$ hybrid consists of the aforementioned hybrid woven fabric enclosing 10 plies of unidirectional graphite tape. The energy-absorption capability of the $[\pm 45^{H}_{F}]_2$ is approximately the average of the $[\pm 45_T]_6$ Gr/E and K/E materials and the hybrid material also has post-crushing integrity. These results suggest that the hybrid material could be a direct replacement for Kevlar, both improving the energy-absorption capability and possessing post-crushing integrity. The $[+45^{H}_{F}/0^{Gr}_{5T}]_S$ hybrid material has an energy-absorption capability that exceeds all Gr/E layups evaluated and is 25 percent greater than 6061-T6 aluminum. This hybrid also has post-crushing integrity.

Effects of Specimen Geometry and Scalability

To date there is no standard test specimen or test method for characterizing the energy-absorption capabilities of composite materials. To quantify the energy-absorption capability of composites tubular specimens have been employed. However, the geometry (i.e., characteristic dimension, wall thickness, and cross sectional shape) of these specimens can significantly affect energy-absorption capability. Understanding the effects of specimen geometry is important for predicting the energy-absorption capability of subfloor beam structure.

A series of studies, references 11 and 12, were conducted using circular and square cross section tube specimens fabricated with Gr/E and K/E. Tube ply orientations were $[\pm 45]_N$. This ply orientation is used in typical subfloor beam structure. Circular cross section tube diameters ranged from 1.27 cm to 10.16 cm. The number of ±45 ply pairs (N) was between 2 and 24 resulting in internal diameter-to-wall thickness (D/t) ratios of 1.4 to 125. The energy-absorption trends for the circular cross section tube specimens are shown in figures 16 and 17. The energy-absorption capability of Gr/E circular cross section tubes is a nonlinear function of tube D/t ratio. All Gr/E tubes exhibited a progressive brittle fracturing crushing mode. A significant finding was that each diameter tube produced a different nonlinear response. A reduction in tube D/t ratio results in an increase in energy-absorption capability. This increase in energy-absorption capability is related to a reduction in interlaminar cracking in the crushed region of the tube. As the length and number of interlaminar cracks decreases, the buckling load of the associated lamina bundles increases. These results suggest that as D/t ratio decreases the sustained crushing stress approaches the compressive strength of the material. Therefore, the energy-absorption potential of a composite material is its compressive strength.

The K/E circular cross section tubes also exhibited a nonlinear energy-absorption capability as a function of tube D/t ratio as depicted in figure 17. Unlike the Gr/E tube results, the K/E test results do not show a different energy-absorption capability as a function of tube inside diameter. When

crushed, all K/E tubes, exhibited the characteristic local buckling crushing mode. The buckle wave length varied with tube geometry (tube diameter and wall thickness).

The nonlinear variation in energy-absorption capability with D/t ratio is similar to the classic short wave length buckling response of axially compressed metallic cylinders. Closed form buckling equations for metallic cyclinders predict a linear variation in buckling load with D/t ratio, although tests yield a quadratic behavior. The differences between test and analytical predictions are generally attributed to inelastic behavior of the material and local imperfections.

Kevlar fibers exhibit inelastic compressive behavior similar to that of metallic materials. The nonlinear response with respect to D/t ratio is partially attributed to the fibers' inelastic response and tube imperfection. The increase in energy-absorption capability as D/t ratio decreases is related to a decrease in interlaminar cracking. The decreased interlaminar cracking reduces the magnitude of the local imperfections which directly affects the buckling load and, hence, the energy-absorption capability.

Square cross section Gr/E and K/E tubes with ply orientations of $[\pm 45]_N$ were also evaluated. The results are depicted in figures 18 and 19. The inside tube widths ranged from 1.27 cm to 7.62 cm. The number of ±45 ply pairs (N) were between 2 and 8 resulting in tube width-to-wall thickness ratios of between 6 and 125. The energy-absorption capability of Gr/E tubes is a nonlinear function of W/t ratio. Generally, as W/t ratio decreased the energy-absorption capability increased and reached a maximum between W/t ratio of 20 and 55. With further decreases in W/t the energy-absorption capability decreased. The predominant crushing mode was a lamina bending mode or a combined brittle fracturing and lamina bending mode. All Gr/E tubes also exhibited a laminate tearing mode at the corners of the tubes. Square cross section tubes had lower energy-absorption capability than comparable size circular cross section tubes.

The energy-absorption capability of K/E square cross section tube specimens is a nonlinear function of tube W/t ratio as depicted in figure 19. This trend is similar to that of circular cross section tube specimens. The increase in energy-absorption capability with respect to decreasing W/t ratio is related to the reduced interlaminar cracking and is consistent with the buckling load characteristic of edge supported plates.

All of the K/E specimens crushed in a progressive local buckling mode. The buckle wave length is a function of tube geometry (width and wall thickness). The magnitude of the variation of the crushing force was a function of W/t ratio. The greater the W/t ratio the greater the variation in crushing force.

Tube specimens were geometrically scaled by proportionally changing tube inside diameter or width and wall thickness. If the energy-absorption capability of these tubes were geometrically scalable, tube specimens that have the same D/t or W/t ratio, although different diameters or widths and thicknesses, should have similar energy-absorption capabilities. The test results shown in figures 16-19 suggest the energy-absorption capability of Gr/E tubes was not geometrically scalable while the energy-absorption capability of K/E tubes was scalable.

Effects of Crushing Speed

Tests were conducted, reference 4, to investigate whether the energy-absorption capability of Gr/E and K/E composite materials is a function of crushing speed. Tube specimen ply orientations were $[0/\pm\theta]_2$ and $[\pm\theta]_3$. Figures 20 and 21 present the test results for crushing speeds between 10^{-5} m/sec and 12 m/sec. The energy-absorption trends varied for the different materials and ply orientations evaluated.

The energy-absorption capability of $[0/\pm\theta]_2$ Gr/E specimens was not influenced by crushing speed. All specimens crushed in a brittle fracturing mode. In the brittle fracturing mode the energy associated with the fracturing of the lamina bundles is considerably more than the energy associated with interlaminar crack growth. The 0 degree plies reduced strain rate effects in the mechanical response of the lamina bundles. Therefore, the energy-absorption capability of $[0/\pm\theta]_2$ specimens should not be a function of the crushing speed.

The energy-absorption capability of $[\pm\theta]_3$ Gr/E specimens was a function of crushing speed. As ply orientation angle, θ, increased from 15 to 75 degrees the magnitude of the effects of crushing speed on energy-absorption capability increased. Energy-absorption capability increased as much as 15 percent over the speed ranged tested. All $[\pm\theta]_3$ specimens crushed in predominantly a brittle fracturing mode. As the ply orientation angle increased from 15 to 75 degrees the mechanical response of the lamina bundles became more strongly influenced by the matrix properties than by the fiber properties. Correspondingly, the percent of the total energy absorbed by the fracturing of the lamina bundles decreased. Therefore, the energy absorbed by the interlaminar crack growth relative to the total energy absorbed increased. Thus, the energy-absorption capability of the $[\pm\theta]_3$ Gr/E specimens are a function of crushing speed and ply orientation.

Figure 21 shows the effect of crushing speed on the energy-absorption capability of $[0/\pm\theta]_2$ and $[\pm\theta]_3$ K/E tube specimens. All K/E tube specimens crushed in the local buckling mode. The energy-absorption capability of K/ E is a function of crushing speed, particularly between 6 m/sec and 12 m/sec. Energy-absorption capability increased between 20 and 40 percent for both $[0/\pm\theta]_2$ and $[\pm\theta]_3$ specimens between crushing speeds of 10^{-5} m/sec and 12 m/sec. Specimens with fibers predominantly oriented in the direction of the applied load (e.g., $[0/\pm15]_2$ and $[\pm15]_3$) exhibited the most significant increase in energy-absorption capability as crushing speed increased from 6 m/sec to 12 m/sec. The mechanical response of Kevlar fibers is a function of strain rate, therefore, the observed changes in energy-absorption capability are reasonable.

The results describing the effect of crushing speed are consistent with the crushing process described in a previous section. Energy-absorption capability is a function of crushing speed when the mechanical response of the controlling crushing mechanisms is a function of strain rate.

COMPOSITE SUBFLOOR BEAM CONCEPTS FOR ENERGY ABSORPTION

Four different subfloor beam concepts have been evaluated; sandwich, sine wave and two integrally stiffened concepts. The subfloor beam concepts are shown

in figure 22 and details are available in reference 13. In this section the relative energy-absorption capabilities of the different concepts are discussed. The energy-absorption trends of the beams are compared with the material response based upon tube tests. Finally, a method to predict the energy-absorption capability of composite subfloor beams is presented.

Energy Absorbing Subfloor Beam Concepts

The sandwich beams evaluated were fabricated using Nomex honeycomb core co-cured to K/E woven fabric face sheets oriented at ±45 degrees. Different through-the-thickness stitching concepts were also evaluated. The energy-absorption capability test results are shown in figure 23. The stitching did not significantly affect the energy-absorption capability. However, the stitching did improve crushing load uniformity. The sandwich concepts crushed in the characteristic local buckling mode and they exhibited post-crushing integrity. The combinations of stitching parameters (i.e., stitch spacing, stitch pattern, and thread size) investigated was not exhaustive. Other stitching parameters might improve energy-absorption capability. However, the energy-absorption capability of the sandwich beams was significantly lower than other concepts.

The evaluation of sine-wave beams involved many different materials, material forms, hybridization, ply orientations and geometries (D/t). The sine-wave concepts were tangent half tube (included angles of 180 degrees) designs. A limited number of results will be presented here. The energy-absorption trends of sine-wave beams are similar to those trends found for circular cross section tube specimens. The effects of beam geometry for K/E beams are compared with tube data in figure 24. The agreement between beam and tube results is excellent. Beam and tube results for hybrid materials, as shown in figure 25, were equally good. The crushing modes of Gr/E and K/E beams are shown in figure 26. These crushing modes are similar to crushing modes of comparable tube specimens. The sine-wave beam concept was the most efficient energy absorbing concept evaluated. The energy-absorption efficiency is related to the relative efficiency between the circular and flat sections.

Both circular and rectangular tube stiffened beams were evaluated. Beams were fabricated from Gr/E, K/E and 6061-T6 aluminum. Ply orientation of the composite beams were $[(\pm 45)_4]_S$ and beam thickness was comparable for composite and aluminum beams. Different geometry stiffened beams were evaluated to compare energy-absorption trends with results from tube data. Figures 27 and 28 depict the test results for these beam concepts. For beams of comparable geometry the Gr/E beams had higher energy-absorption capability than Kevlar or aluminum beams. Energy-absorption capability as a function of beam geometry for both Gr/E and K/E was consistent with that determined from tube tests. That is, as D/t or W/t increased the energy-absorption capability decreased. The crushing modes of the beams were also consistent with the modes of tube specimens of the same material. As seen in figure 29 the K/E specimens crushed in a local buckling mode while the Gr/E specimens exhibited a brittle fracturing mode along the curved sections and a lamina bending mode in the flat sections.

Method of Predicting Energy Absorption Capability

Tests established that the crushing characteristics and energy-absorption trends of beams and tube specimens are similar. These results suggest that the energy-absorption capability of a beam can be predicted using tube data.

A method was formulated, reference 14, for predicting the energy-absorption capability of structural elements. The hypothesis is: the crash energy-absorption capability of a structural element is the sum of the weighted average of the energy-absorption capability of its characteristic elements. Mathematically, in terms of the specific sustained crushing stress (σ/ρ), this can be expressed as

$$(\sigma/\rho)_{S.E.} = \sum_{i=1}^{n} \frac{A_{i_{C.E.}}}{A_{S.E.}} * (\sigma/\rho)_{i_{C.E.}} \qquad (1)$$

This hypothesis assumes the structure is properly designed to crush prior to catastrophic failure. Other requirements are that the tube specimens must have the same D/t or W/t ratio as the characteristic elements of the beam, the same ply orientation and stacking sequence, and have the same material form (e.g., tape, woven, filament wound).

This prediction method has been verified using several Gr/E, K/E and hybrid sine wave and stiffened beams. A detail example of this prediction method is given for a circular cross section tube stiffened beam fabricated with K/E. Figure 30 shows the beam configuration and dimensions. Web width between tube stiffeners was 3.81 cm and web thickness was 0.20 cm resulting in a W/t ratio of 19. The cross sectional area of each web was 0.76 cm^2. The web extended beyond the stiffeners 1.27 cm on each side of the beam. The W/t ratio of the web beyond the stiffeners was 6 and cross sectional area was 0.25 cm^2. The composite layup in the web region was $[\pm 45]_{3S}$. The stiffener was a circular tube with an inside diameter of 2.54 cm and a wall thickness of 0.09 cm resulting in a D/t ratio of 28.2. The layup of the tube was $[\pm 45]_3$, and the cross-sectional area was 0.78 cm^2. Using equation 1 to compute the energy-absorption capability of the beam with the appropriate circular and square cross section tube data results in

$$(\sigma/\rho)_{S.E.} = (4*A_{Tube}*(\sigma/\rho)_{Tube} + 3*A_{Web}*(\alpha/\rho) + 2*A_{End\ of\ Web}*(\sigma/\rho)_{End\ of\ Web})/A_{S.E.},$$

$$(\sigma/\rho)_{S.E.} = 30 \text{ Nm/gr.}$$

The measured energy-absorption capability of the beam was 28 Nm/gr. The difference between the predicted and measured values was approximately 7 percent.

Development of efficient energy absorbing concepts requiring a minimum number of design support tests for validation should now be readily achievable using the previously described prediction method. The application of the prediction method should result in a reduction in design cost and result in a lighter structure.

Composite material and structure can be tailored for efficient energy-absorption. However, additional work is required to advance this technology to the existing level for other composite structure. Further development of energy absorbing subfloor beam intersections and crushing initiators is required. Also, studies are needed, similar to those in references 15 and 16, are needed to incorporate energy absorbing structural concepts into fuselage sections to reduce manufacturing cost and reduce other development risks.

COMPOSITE FUSELAGE FRAME STRUCTURE

The subfloor structure previously discussed absorbs the energy in a crash but does not insure the structural integrity of the fuselage. The integrity of the fuselage must be maintained by the frames, bulkheads, and longerons in the structure. This integrity is important because it provides a protective shell around the occupants preventing foreign object intrusion and collapse of the fuselage. As part of the fuselage structural integrity investigation research on fuselage frames was conducted, reference 17. Drop tests of two aluminum and three Gr/E frames was conducted to investigate the impact acceleration levels and failure mechanisms.

The frame specimens were Z cross section frames approximately two meters in inside diameter. Frame dimensions are shown in figure 31. Each frame was fabricated in quarters and assembled with bolted splice plates. Ten pound masses were attached to both the left and right sides of the frames. Frames were instrumented with accelerometers and strain gages. Frames were dropped from a height of approximately four meters, producing an approximate impact speed of 8.2 m/sec.

Upon impact, the aluminum frames exhibited three sites of significant deformation. A plastic hinge formed to the left of the initial impact point which was on a splice plate. Significant section rotation occurred in the entire frame below the attachment points of the ten pound masses. The failure mechanisms of the aluminum frames were very similar to those of actual fuselage sections. The initial acceleration pulses at the impact point and at the floor frame intersection were on the order of 400 G's and 20 G's, respectively. Durations of the initial pulses were 0.0025 sec. and 0.010 sec. for the impact and the floor intersection points, respectively.

Two of the Gr/E frames were tested in an identical manner to the aluminum frames. Failure in the first two specimens occurred at 15 degrees in a counter clockwise direction from the impact point. The sequence of failure events was failure of the outside flange, failure across the web and finally failure of the inside flange. This complete section fracture might have been avoided by using one of the materials which exhibit post-crushing integrity such as Kevlar or a Kevlar-graphite hybrid. The third Gr/E frame was rotated 45 degrees, to impact halfway between the spice plates. The masses were attached in a similar fashion to the attachments on the first two Gr/E frames. Failure occurred at the point of impact. Overall deformations and

shape of frame were similar to the previous Gr/E frames. Typical accelerations at the impact points were approximately 650 G's and 65 G's at the floor-frame intersections. These accelerations are between 2 and 3 times those of the aluminum frames. Initial impact pulse durations were 0.001 sec. and 0.01 sec. at the impact point and the floor-frame intersection points.

A DYCAST finite element model was developed to predict the dynamic response of the frame structures. The calculated and measured strains agree in the general shape of the distribution; however, the measured strains near the splice plate are lower in magnitude than the predicted strains, as seen in figure 32. At angles below -22.5 degrees and above +22.5 degrees, good strain correlation were obtained between prediction and experiment.

The results of these tests provide needed insight into the failure characteristics of fuselage frames when subjected to simulated crash impacts. The good correlation between analysis and experiment is encouraging because it will allow the designer to reduce the support tests required to validate a concept.

CONCLUDING REMARKS

The U.S. Army-Aerostructures Directorate/NASA Langley Research Center joint research program on crashwothiness of composite helicopter structures has made good progress in understanding how composite materials and structures absorb energy and how structures fail under simulated crash conditions. Through this research program an understanding of the cause/effect relationship of composite material and specimen architectural properties on energy-absorption capability has been developed. Efficient energy absorbing structure can be achieved with graphite/epoxy despite the brittle nature of the material. However, careful attention must be given to design details. Graphite/epoxy structures can be more efficient energy absorbers than either Kevlar or aluminum structures. Sine-wave beams were the most efficient energy absorbing subfloor concepts evaluated. An accurate, yet simple, method of predicting the energy-absorption capability of beams was developed.

Additional developments related to beam intersections, crushing initiators and fuselage integration are still needed. Further enhancements of analysis techniques to predict material and global structural response are also necessary.

REFERENCES

1. Light Fixed and Rotary Wing Aircraft Crashworthiness. Mil-Std-1290, Jan. 1974.

2. Winter, R., Pifko, A. B., and Cronkhite, J. D.: Crash Simulation of Composite and Aluminum Helicopter Fuselages Using a Finite Element Program. AIAA Paper 79-0781, 20 SDM Conference, Apr. 1979.

3. Farley, G. L.: Energy Absorption of Composite Materials. Journal of Composite Materials, vol. 17, May 1983.

4. Farley, G. L.: The Effects of Crushing speed On the Energy Absorption Capability of Composite Material. To be published as a NASA TM 1987.

5. Thornton, P. H.: Energy Absorption in Composite Structures. Journal of Composite Materials, vol. 13, July 1979.

6. Hull, D.: Research on Composite Materials at Liverpool University, Part 2: Energy Absorbing Composite Materials. Physics Technology, vol. 14, 1983.

7. Berry, J. and Hull, D.: Effect of Speed on Progressive Crushing of Epoxy-Glass Cloth Tubes. Institute Physics Conference on the Mechanical Properties at High Rates of Strain, 1984.

8. Cronkhite, J. D., Hass, T. J., Berry, V. L. and Winter, R.: Investigation of the Crash Impact Characteristics of Advanced Airframe Structure. USARTL-TR-79-11, Sept. 1979.

9. Farley, G. L.: Effect of Fiber and Matrix Maximum Strain on the Energy Absorption of Composite Materials. Journal of Composite Materials, vol. 20, July 1986.

10. Farley, G. L., Bird, R. K., and Modlin, J. T.: The Role of Fiber and Matrix in Crash Energy Absorption of Composite Materials. Proceedings of the AHS National Specialists' Meeting on Crashworthy Design of Rotorcraft, April 1986.

11. Farley, G. L.: Effect of Specimen Geometry on the Energy-Absorption Capability of Composite Materials. Journal of Composite Materials, vol. 20, July 1986.

12. Farley, G. L.: Energy-Absorption Capability and Scalability of Square Cross Section Composite Tube Specimens. To be published as a NASA TM, 1987.

13. Farley, G. L.: Crash Energy Absorbing Composite Sub-Floor Structure. Submitted to the American Helicopter Society for publication, 1986.

14. Farley, G. L.: A Method of Predicting the Energy-Absorption Capability of Composite Sub-Floor Beams. To be published as a NASA TM, 1987.

15. Jackson, A. C., Balena, F. J., LaBarge, W. L., Pei, G., Pitman, W. A., and Wittlin, G.: Transport Composite Fuselage Technology - Impact Dynamics and Acoustic Transmission. NASA-CR-4035, Dec. 1986.

16. Cronkhite, J. D. and Berry, V. L.: Investigation of the Crash Impact Characteristics of helicopter Composite Structure. USAAVRADCOM-TR-82-D-14, Feb. 1983.

17. Boitnott, R. L., and Carden, H. D.: Drop Testing and Analysis of Six Foot Diameter Graphite-Epoxy Frames. Proceedings of the AHS National Specialists' Meeting on Crashworthy Design of Rotorcraft, April 1986.

TABLE 1. COMPOSITE MATERIALS USED TO INVESTIGATE EFFECTS OF FAILURE STRAIN ON ENERGY-ABSORPTION CAPABILITIES.

Fiber \ Matrix	934	974	5245	F185	HST-7
T300	X	X	X		
AS4			X		
AS6				X	X
K-49	X	X			

FOUR CRUSHING MODES EXHIBITED BY COMPOSITE MATERIAL

Local buckling

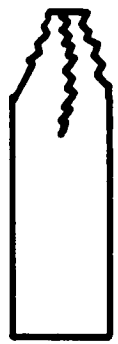

Transverse shearing

Fracturing

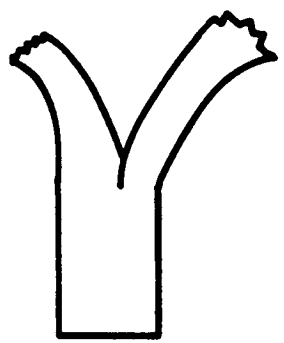

Lamina bending

Figure 1

EFFECT OF FIBER FAILURE STRAIN ON THE ENERGY ABSORPTION OF GRAPHITE REINFORCED COMPOSITE MATERIALS

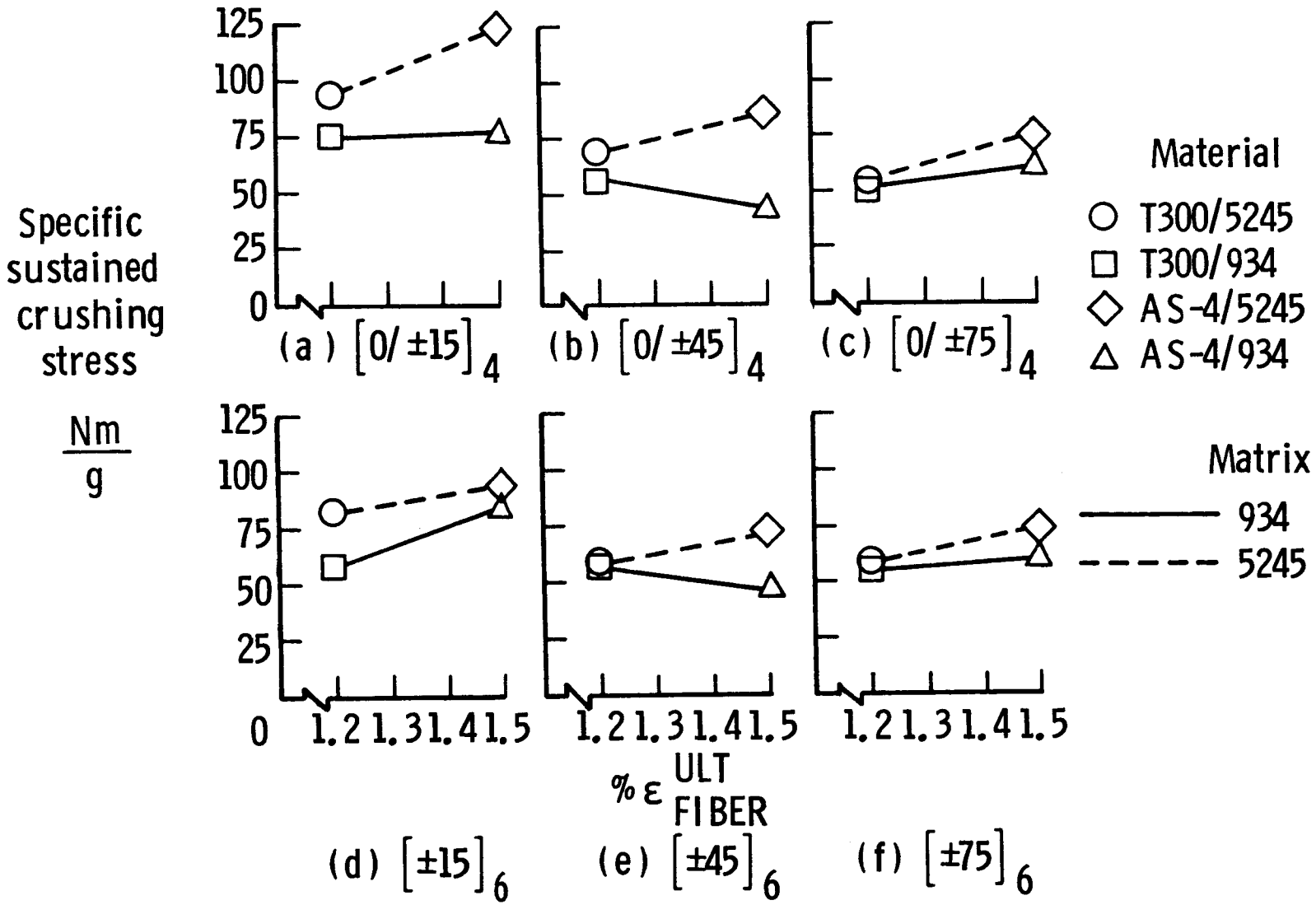

Figure 2

EFFECT OF MATRIX FAILURE STRAIN ON THE ENERGY ABSORPTION OF GRAPHITE REINFORCED COMPOSITE MATERIALS

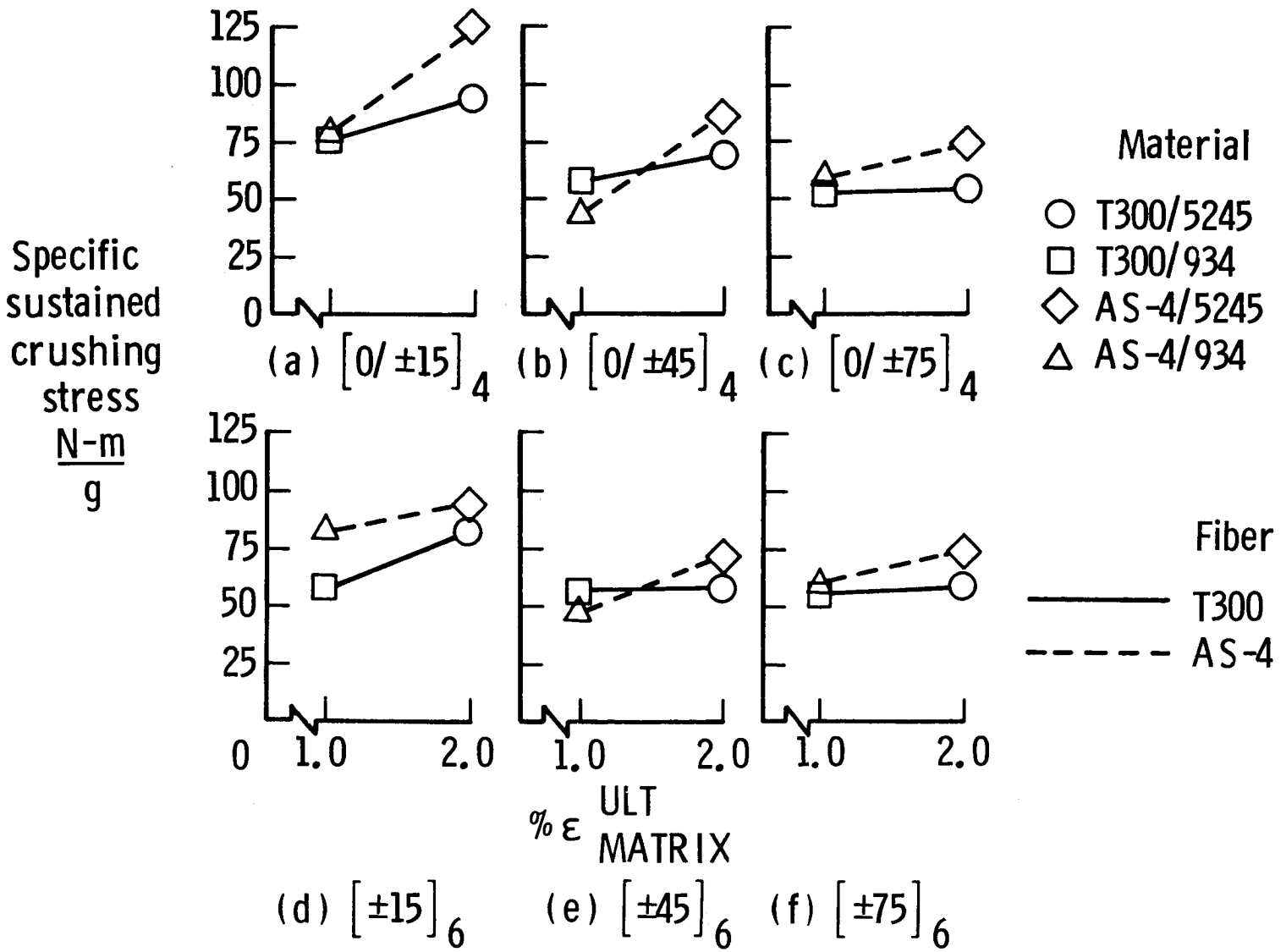

Figure 3

EFFECTS OF FIBER STIFFNESS ON ENERGY ABSORPTION OF $[\pm\Theta]_6$ GRAPHITE/EPOXY COMPOSITE MATERIAL

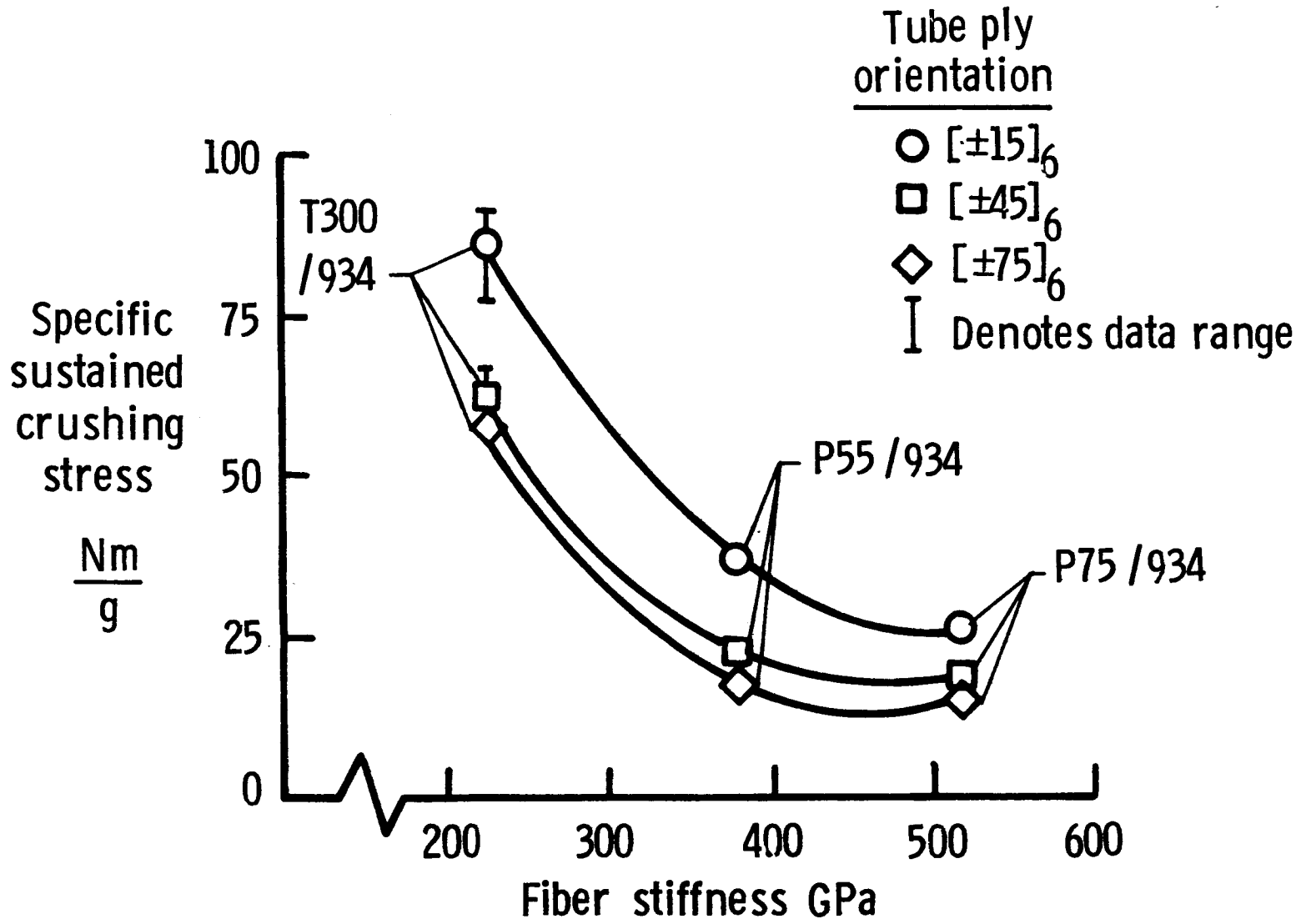

Figure 7

EFFECTS OF MATRIX FAILURE STRAIN ON THE ENERGY ABSORPTION CAPABILITY OF KEVLAR REINFORCED COMPOSITE MATERIAL

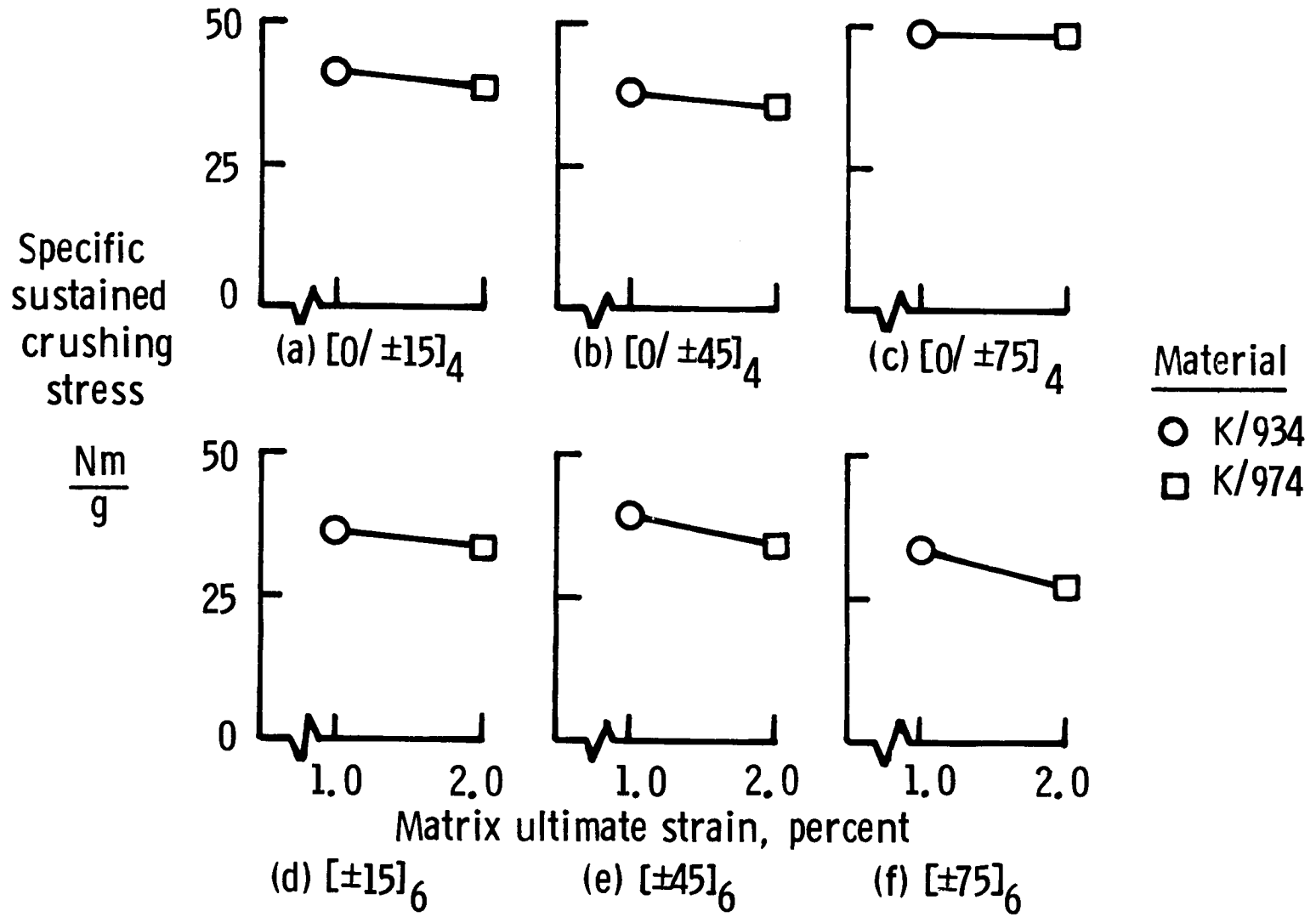

Figure 5

EFFECT OF FIBER AND MATRIX FAILURE STRAIN ON ENERGY ABSORPTION

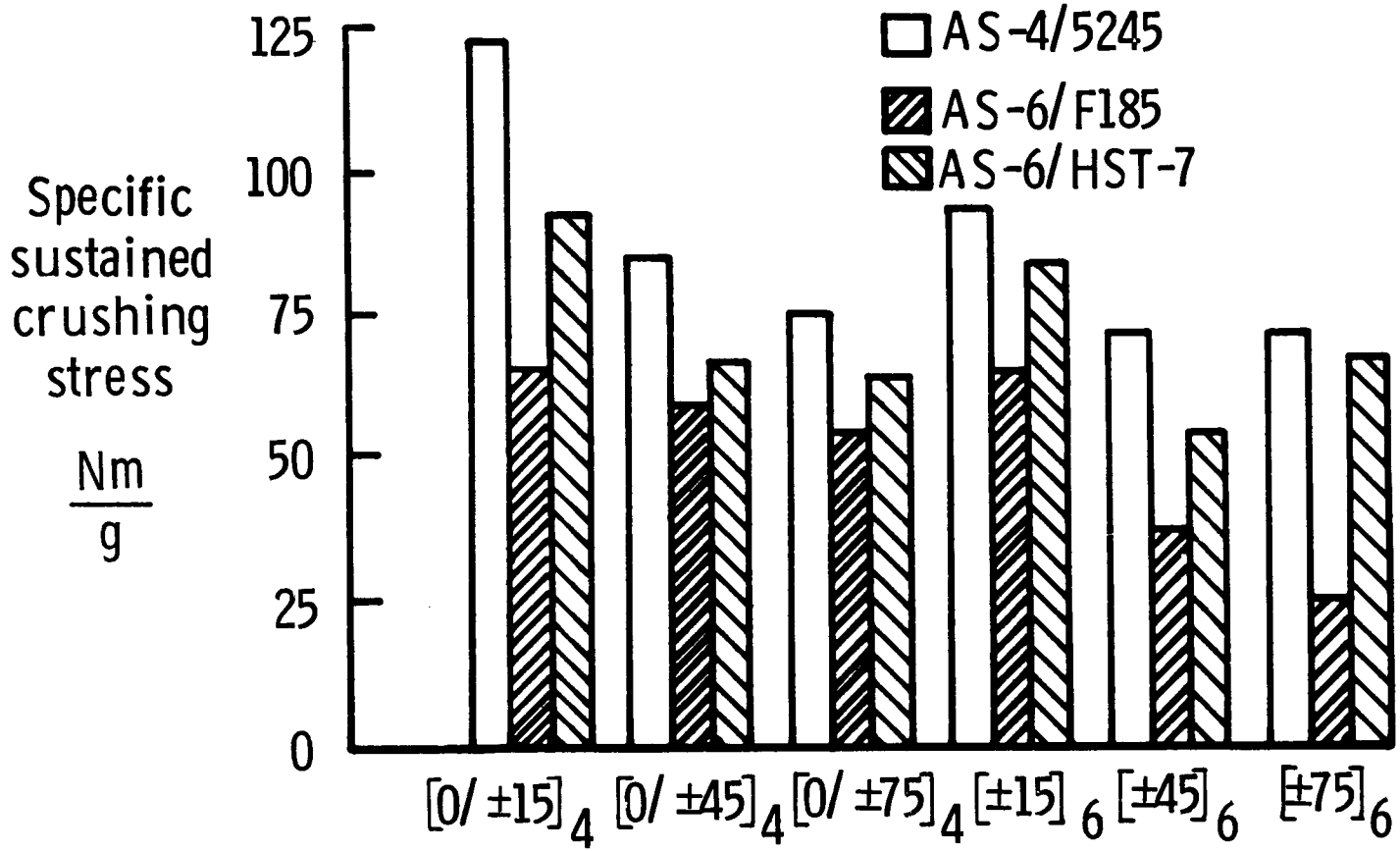

Figure 4

EFFECTS OF FIBER STIFFNESS ON ENERGY ABSORPTION OF $[0/\pm\Theta]_4$ GRAPHITE/EPOXY COMPOSITE MATERIAL

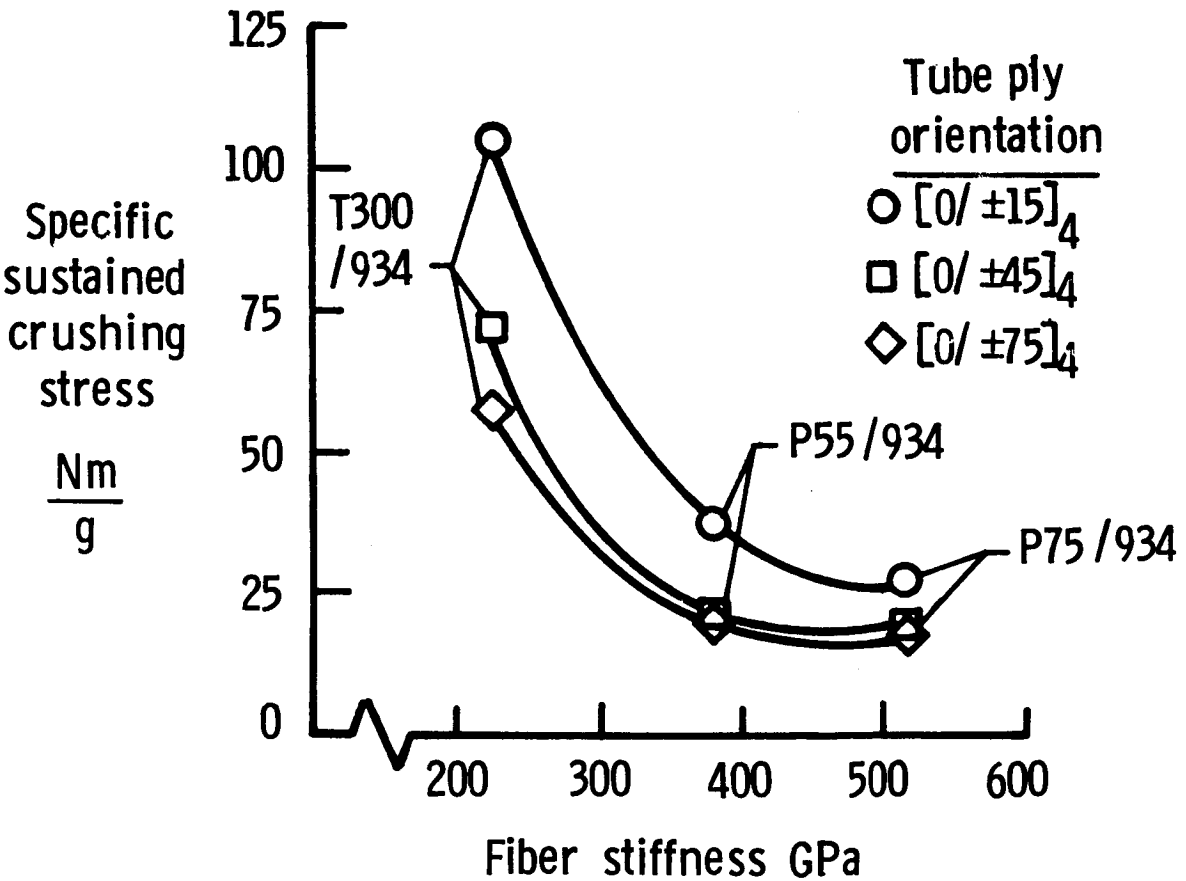

Figure 6

ENERGY ABSORPTION OF Gr/E, K/E, AND Gl/E $[0/\pm\theta]_4$ TUBES

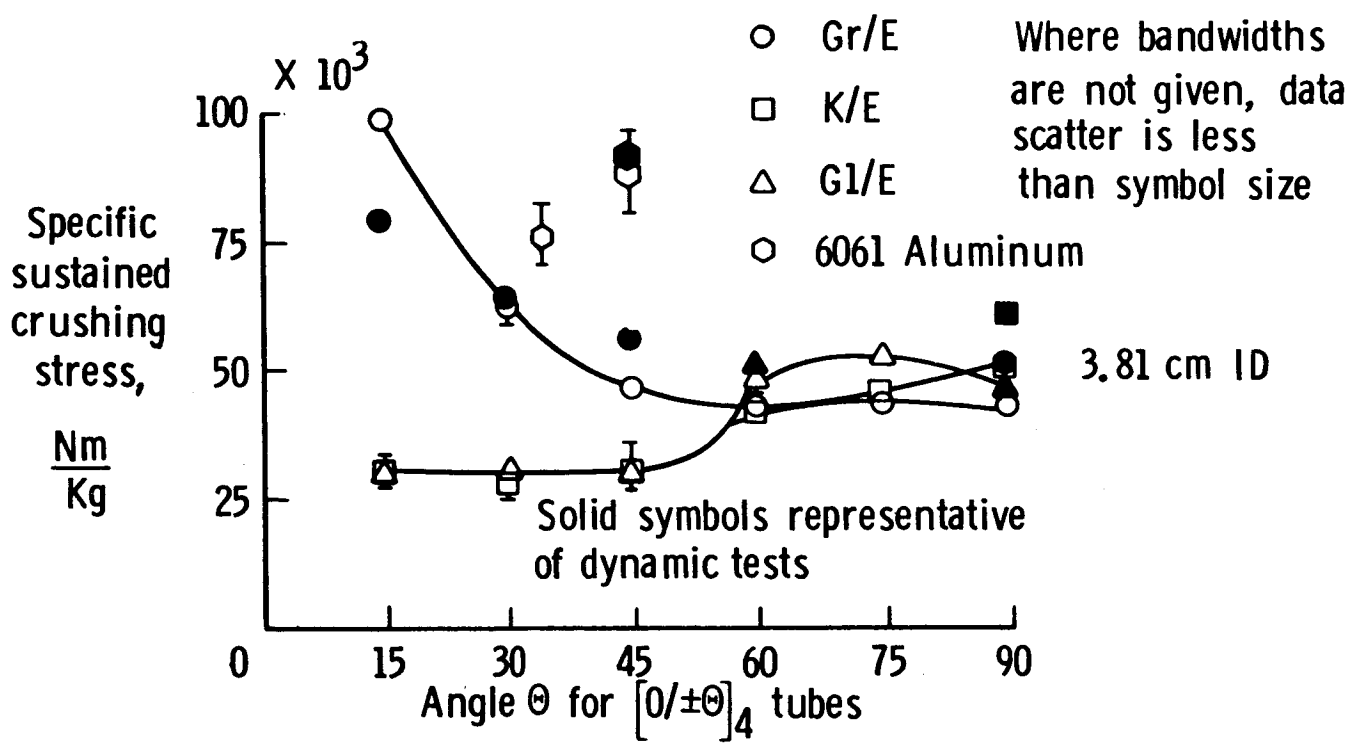

Figure 8

THE EFFECT OF STACKING SEQUENCE ON ENERGY ABSORPTION

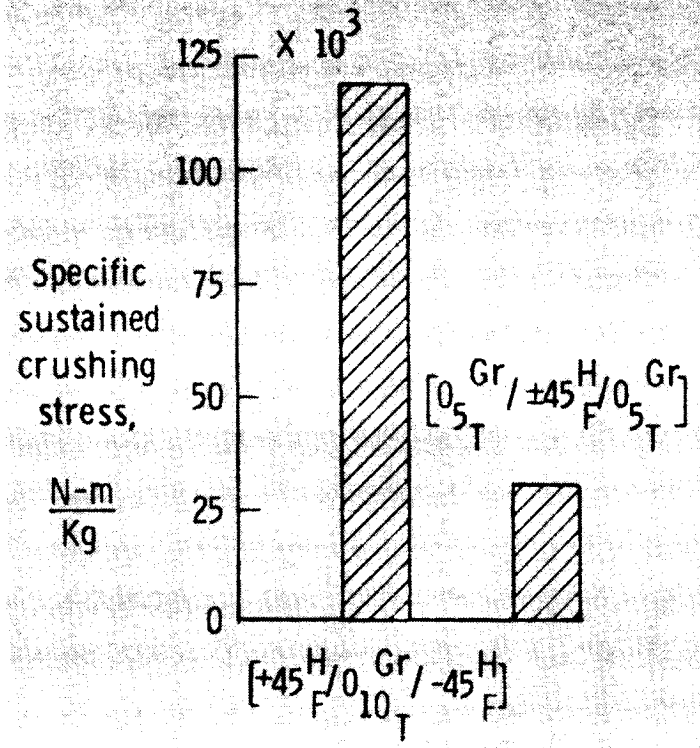

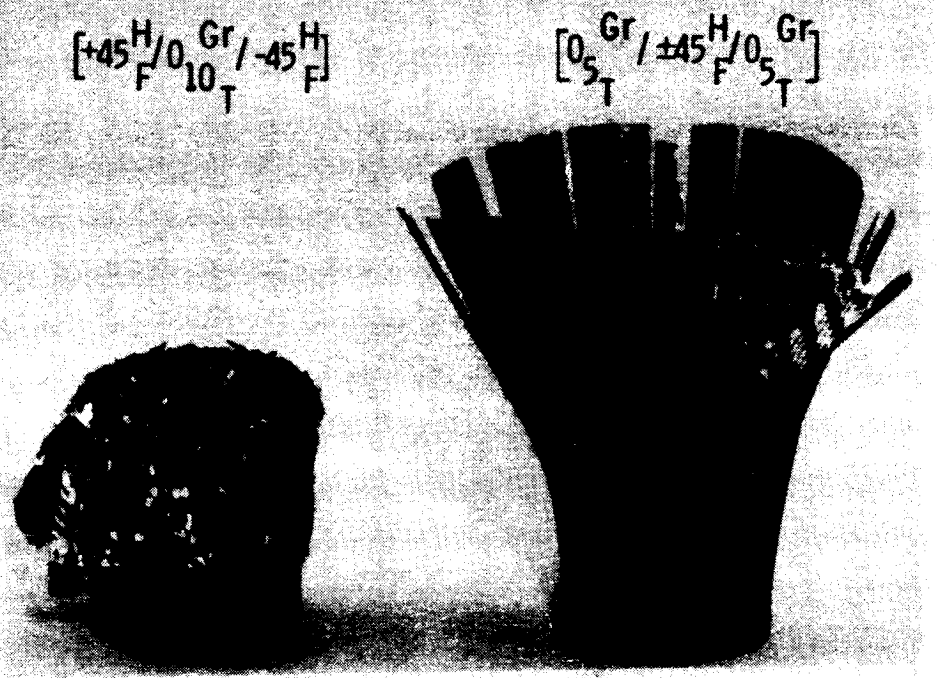

H – Hybrid

Gr – Graphite

T – Tape prepreg

F – Woven fabric prepreg

Figure 9

EFFECT OF STACKING SEQUENCE ON THE ENERGY ABSORPTION OF [±45] COMPOSITE TUBE

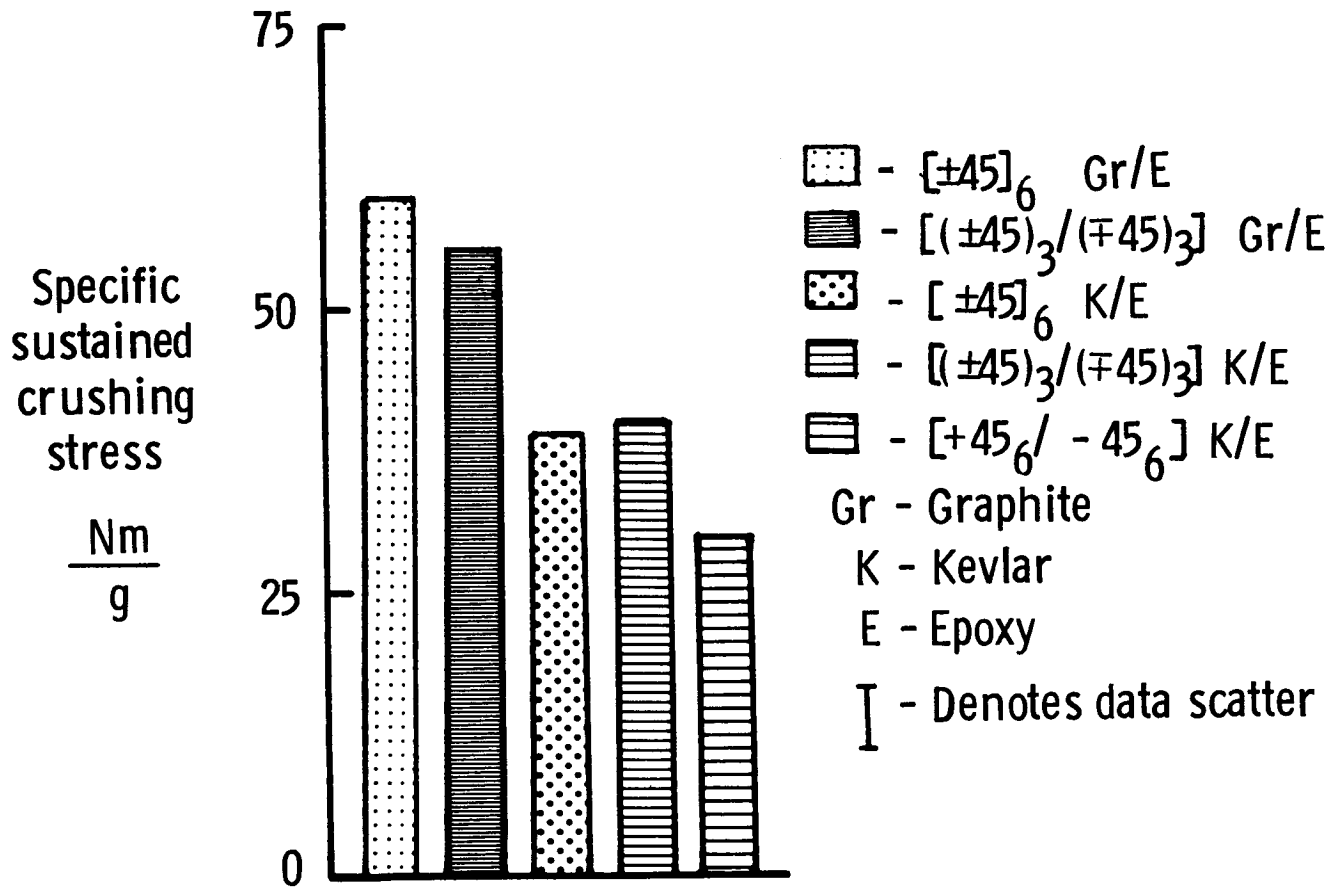

Figure 10

ENERGY ABSORPTION OF $\left[\pm 45\ {}^{K}/O_{N}^{Gr}\right]_{S}$ GRAPHITE-KEVLAR/EPOXY COMPOSITES

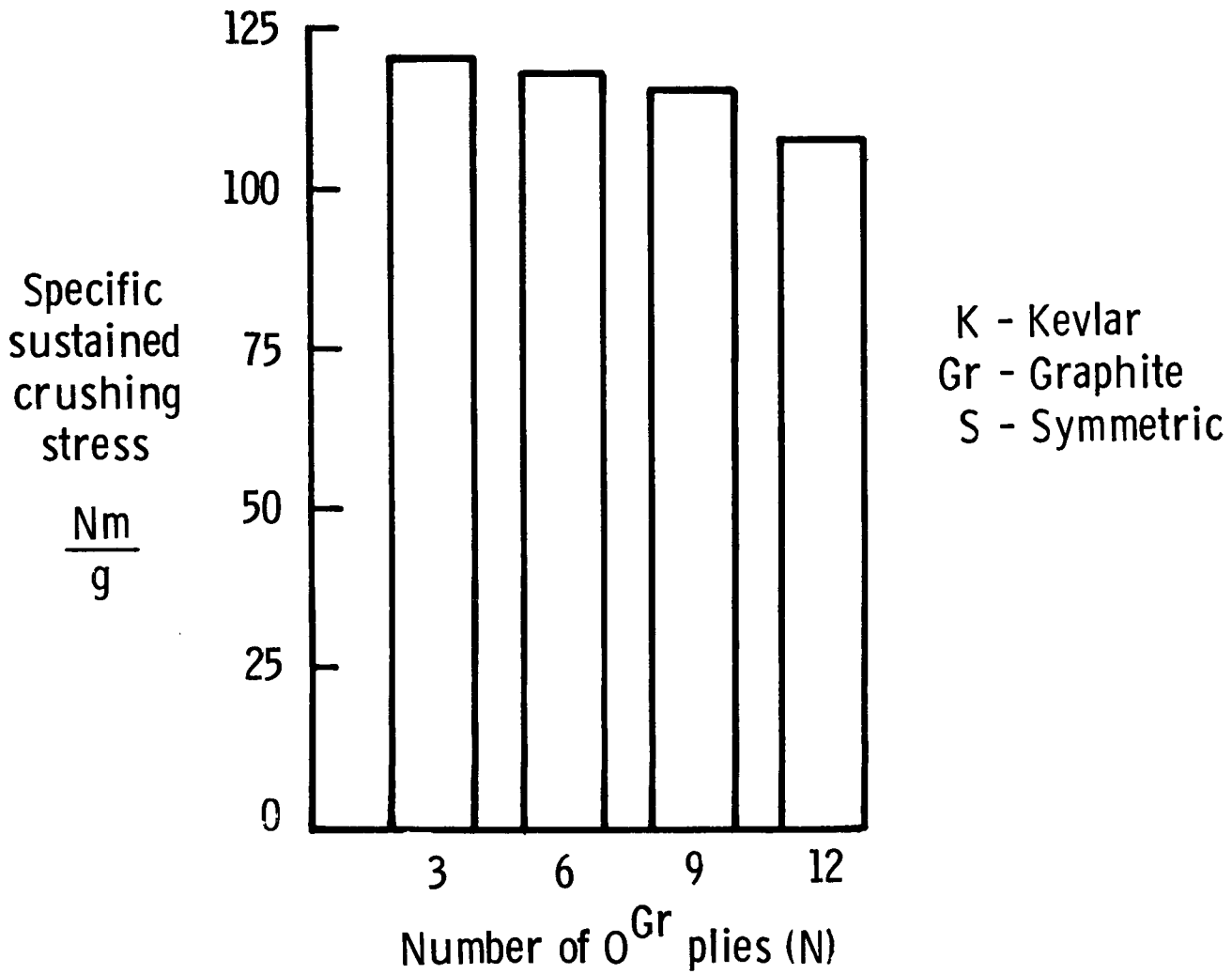

Figure 11

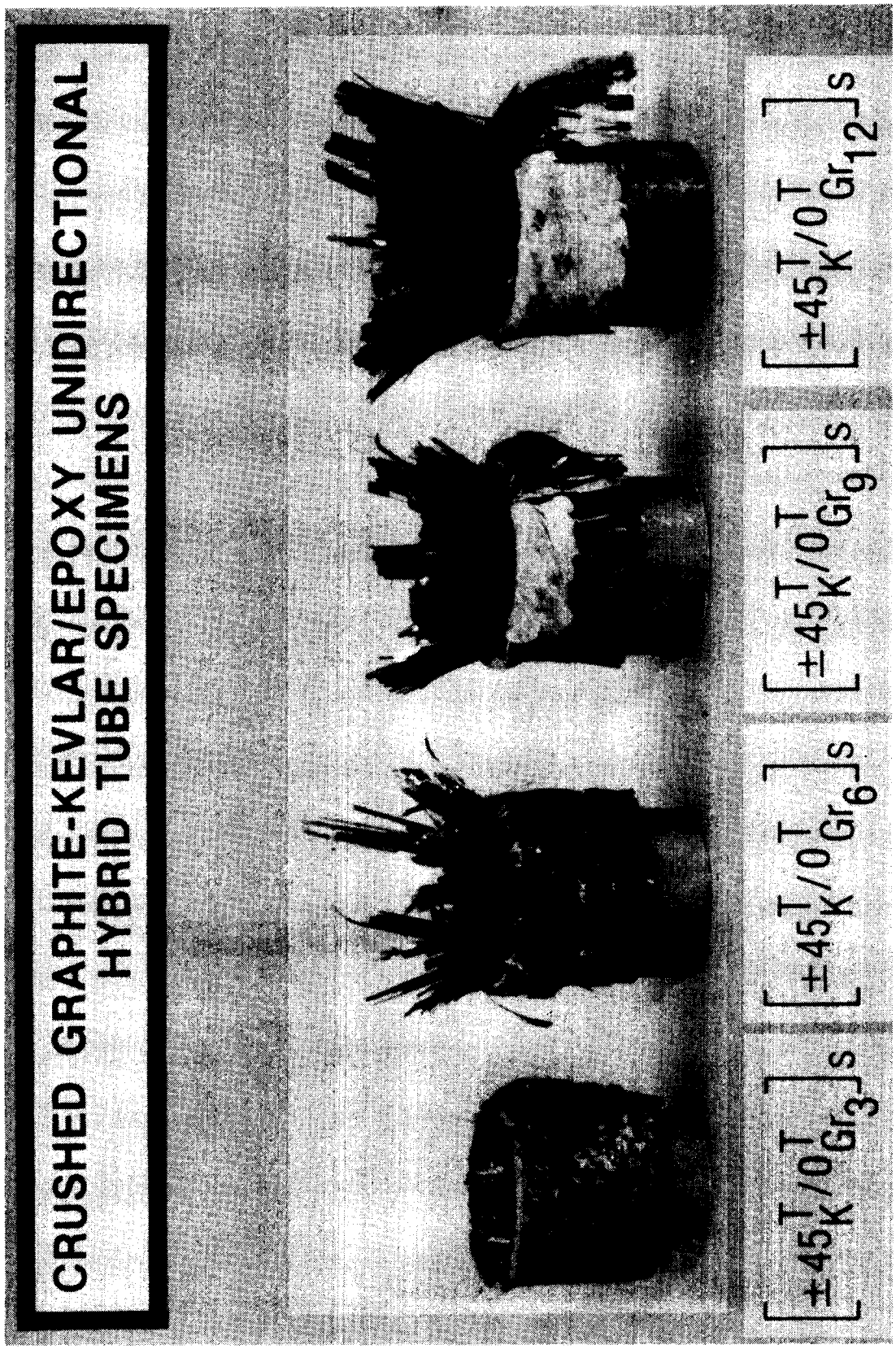

Figure 12

EFFECTS OF FIBER VOLUME FRACTION ON THE ENERGY ABSORPTION CAPABILITY OF T300/934 COMPOSITE MATERIAL

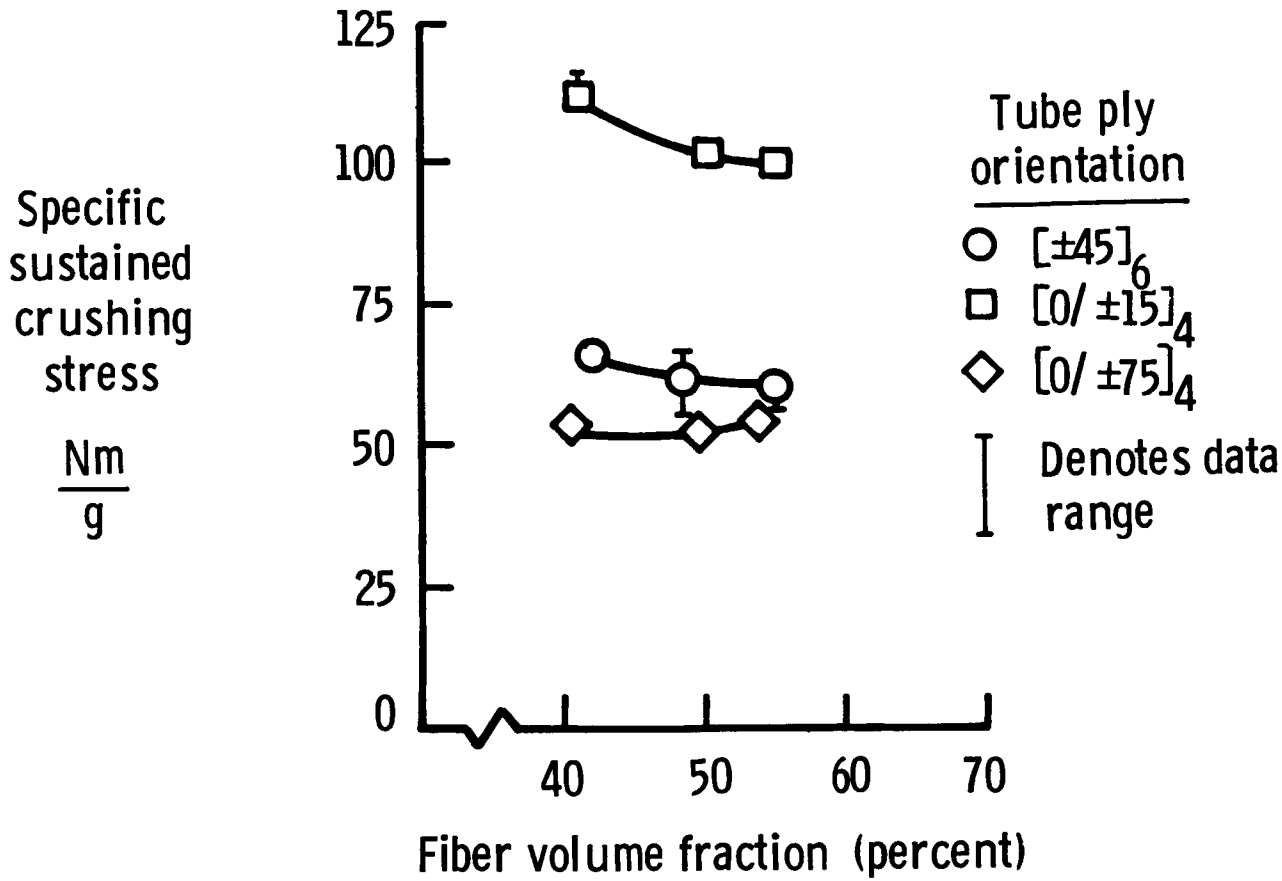

Figure 13

EFFECT OF FIBER VOLUME FRACTION ON THE ENERGY ABSORPTION CAPABILITY OF KEVLAR-49/934 COMPOSITE MATERIAL

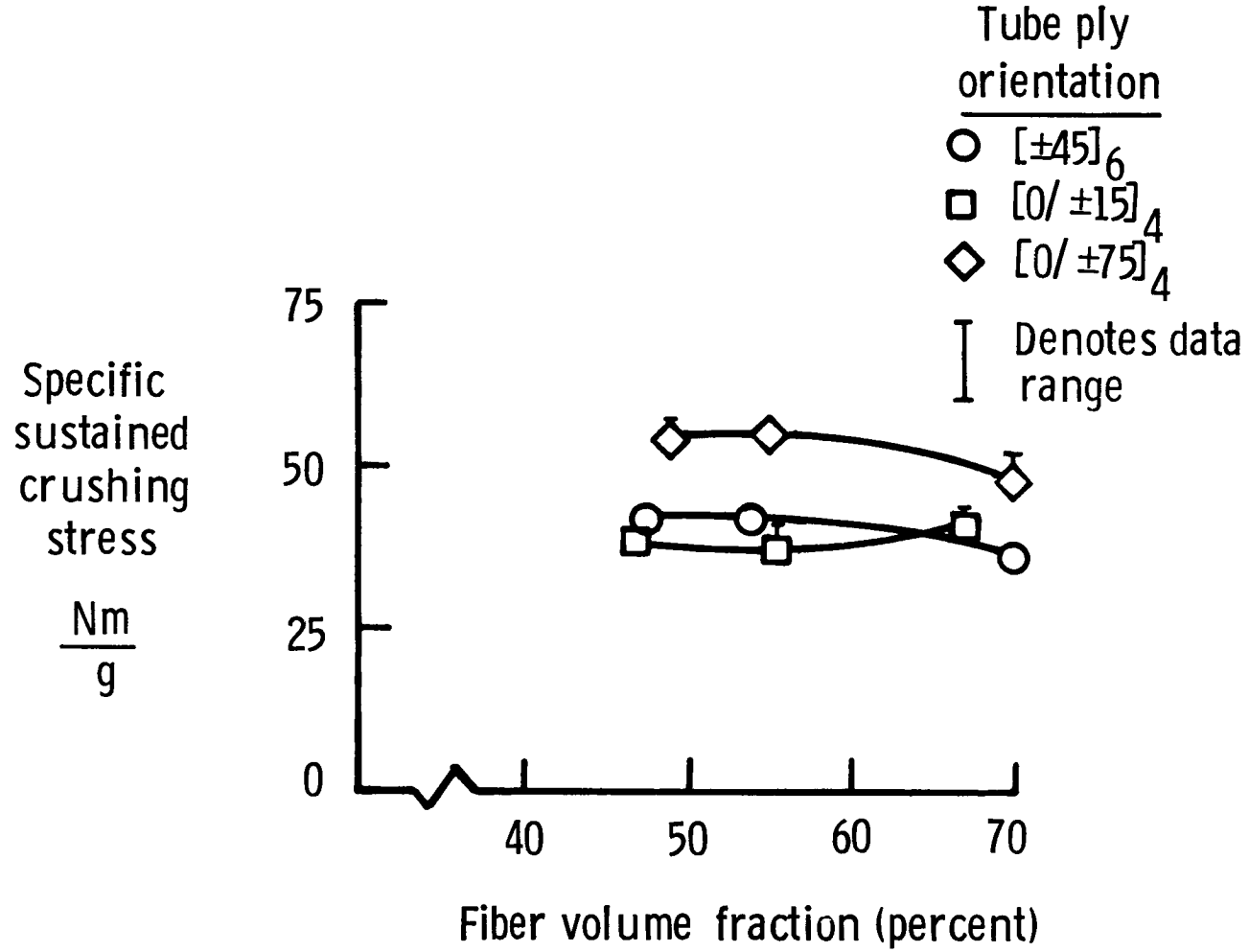

Figure 14

ENERGY ABSORPTION OF GRAPHITE-KEVLAR/EPOXY HYBRID COMPOSITES

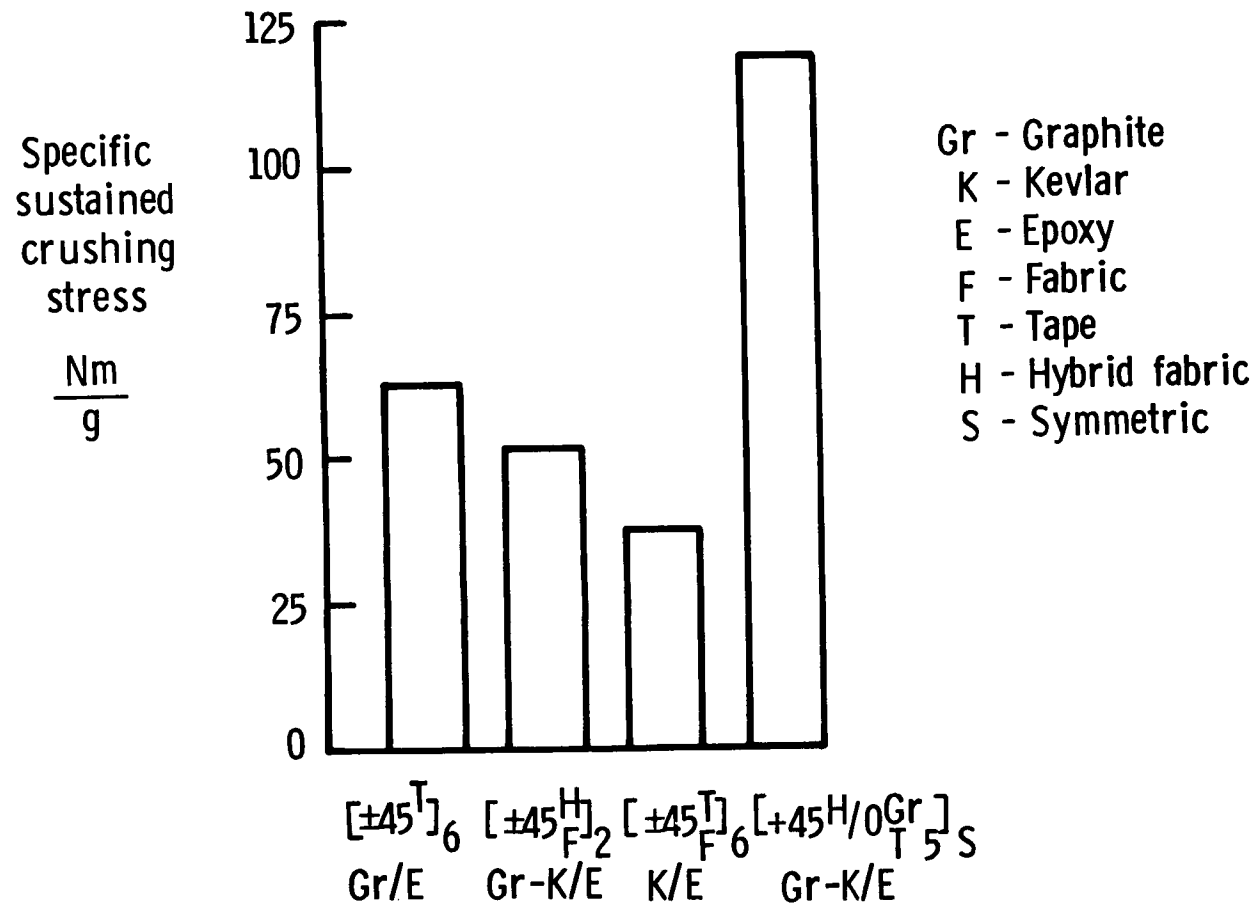

Figure 15

EFFECTS OF D/t RATIO ON THE ENERGY ABSORPTION OF $[\pm 45]_N$ Gr/E TUBES

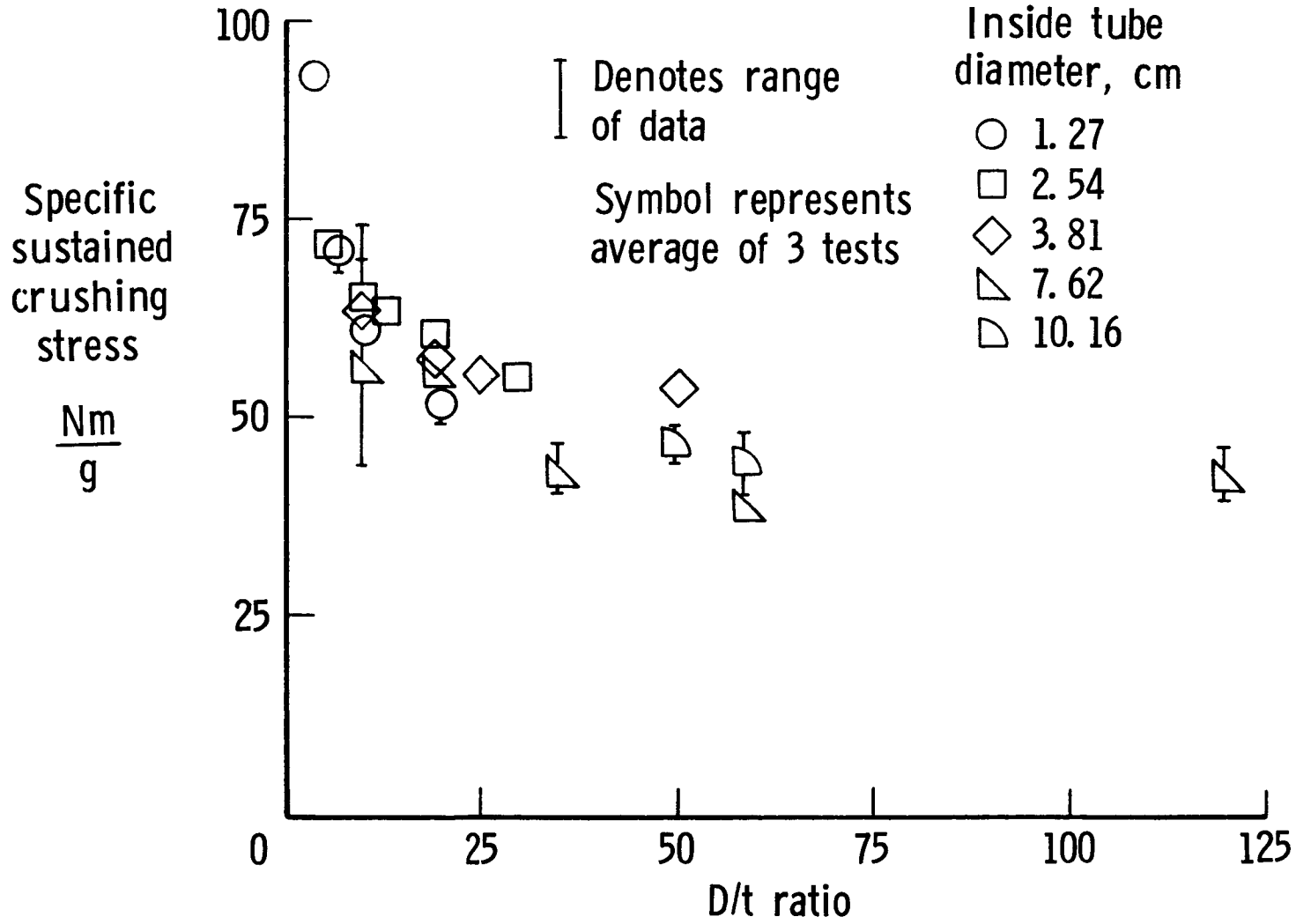

639

Figure 16

EFFECTS OF D/t RATIO ON THE ENERGY ABSORPTION OF $[\pm 45]_N$ K/E TUBES

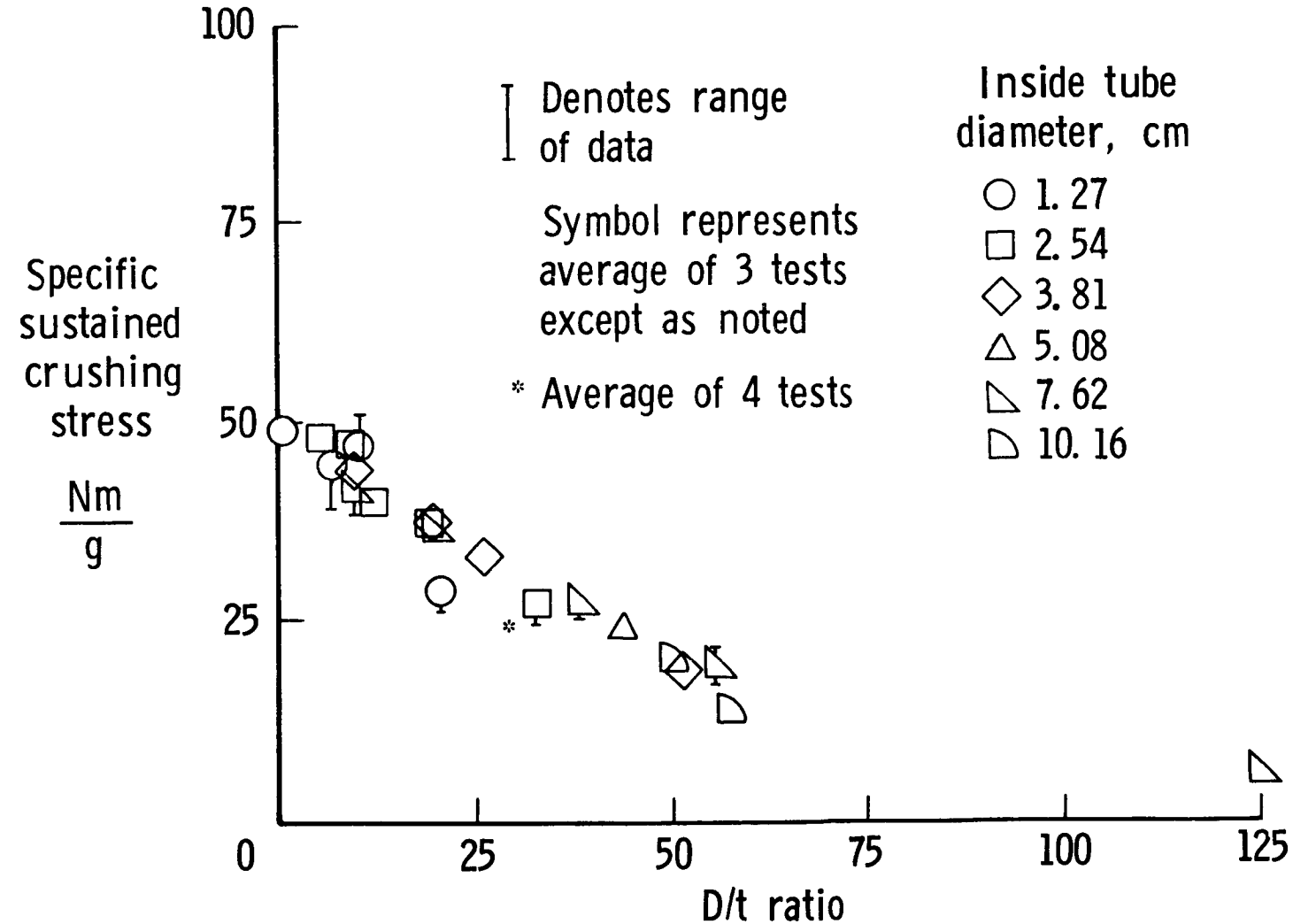

Figure 17

ENERGY ABSORPTION CAPABILITY OF SQUARE GRAPHITE/EPOXY TUBES

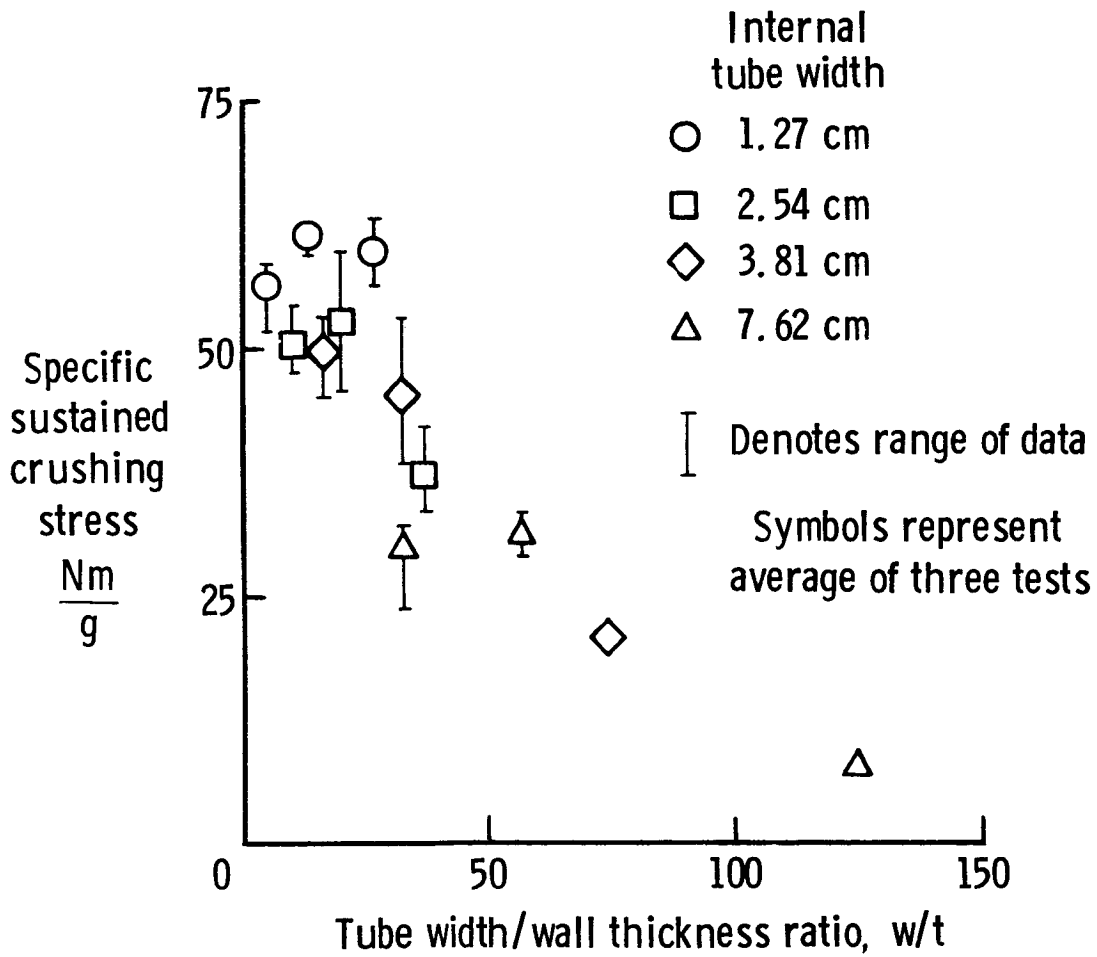

Figure 18

ENERGY ABSORPTION CAPABILITY OF SQUARE KELVAR/EPOXY TUBES

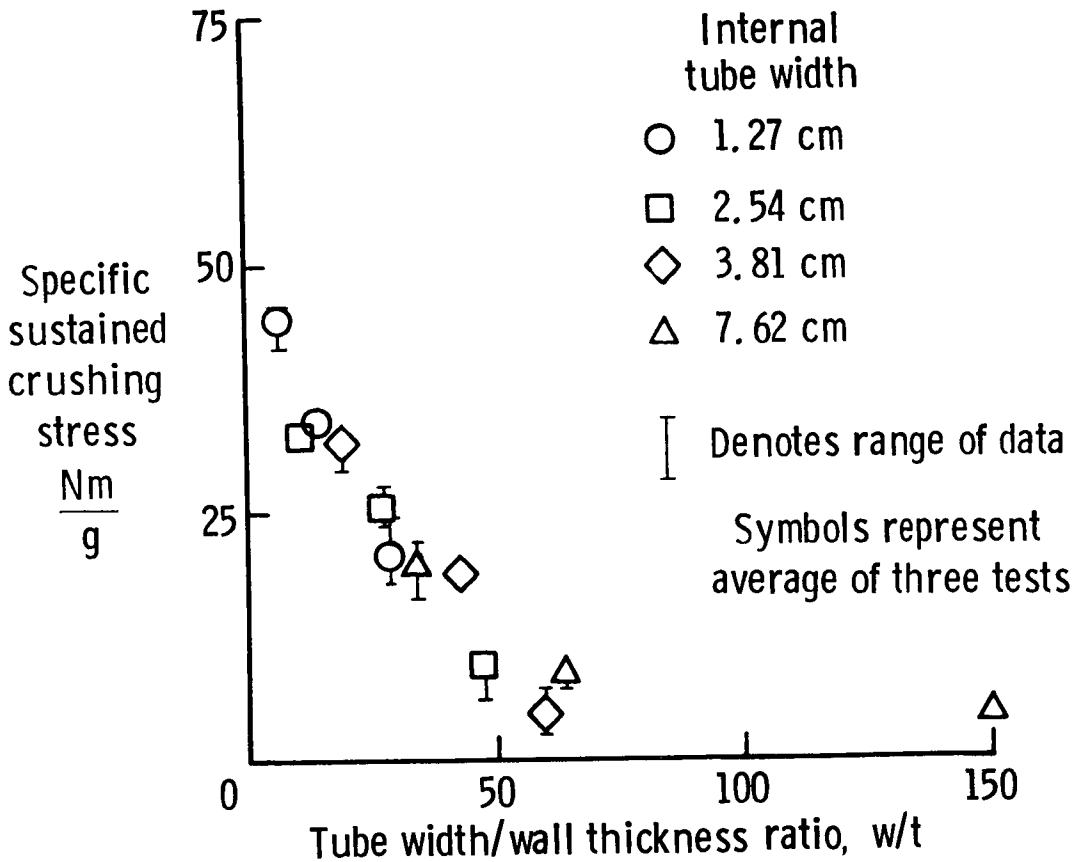

Figure 19

EFFECTS OF CRUSHING SPEED ON Gr/E TUBES

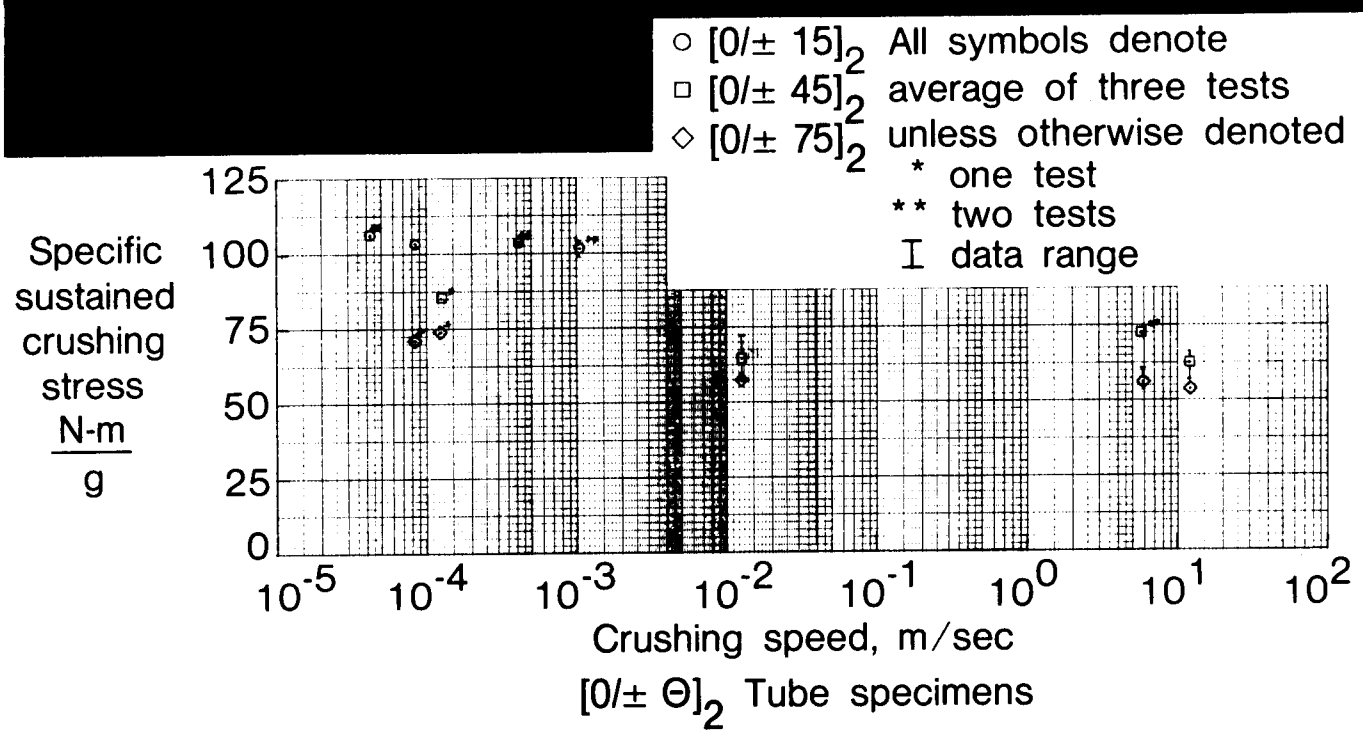

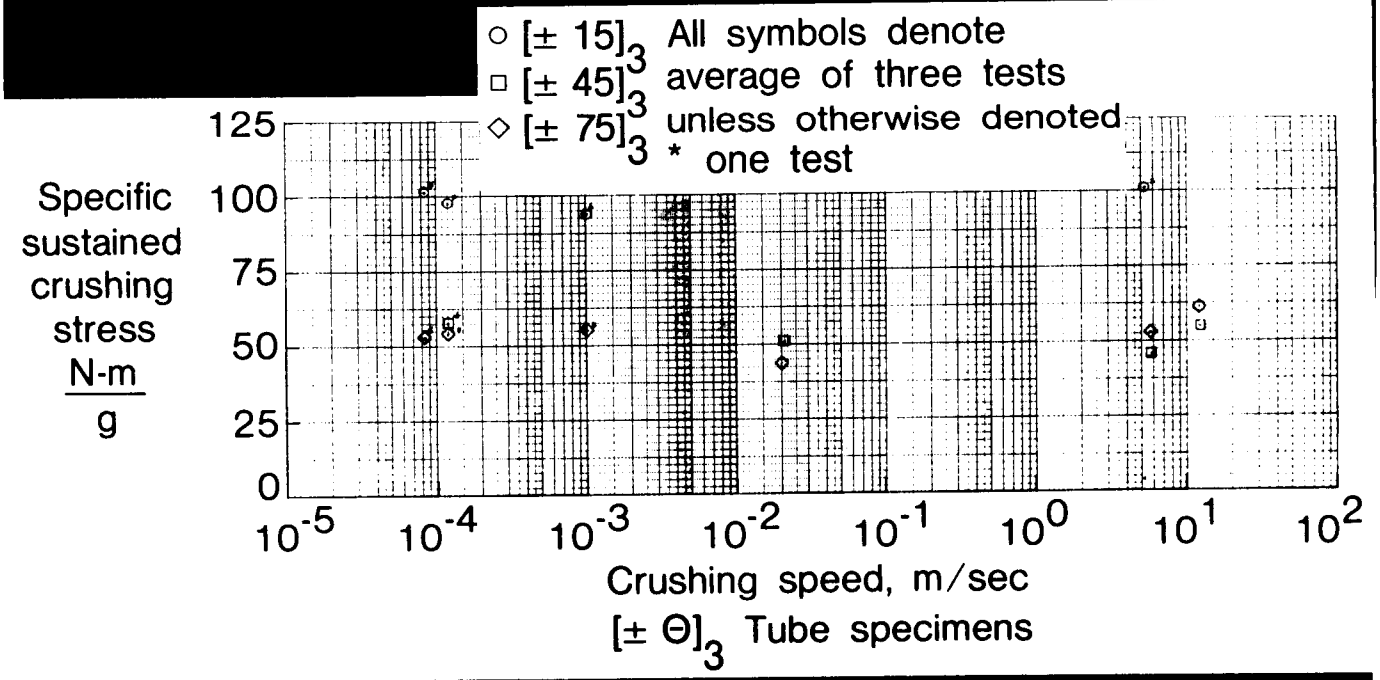

Figure 20

EFFECTS OF CRUSHING SPEED ON K/E TUBES

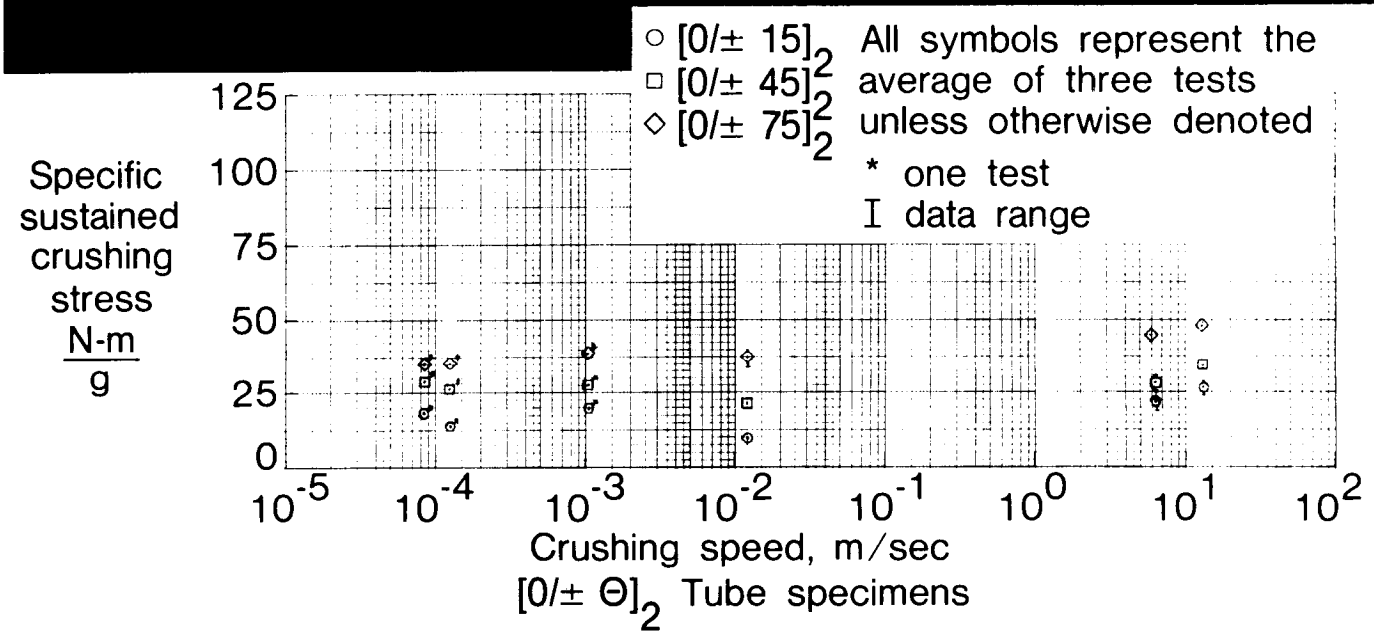

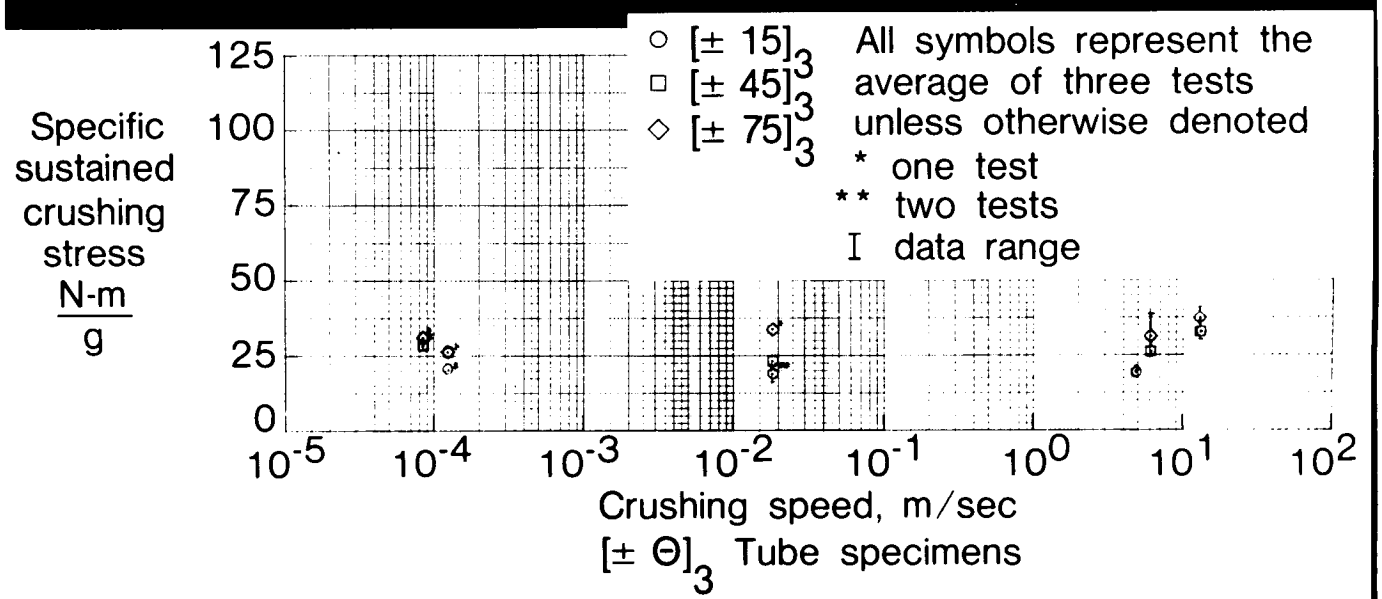

Figure 21

ENERGY ABSORBING BEAM CONCEPTS

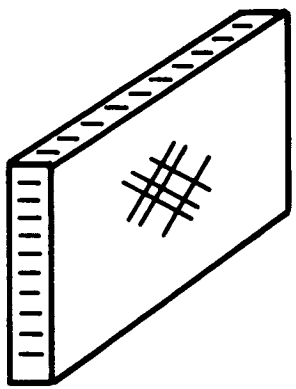

Honeycomb-sandwich beam

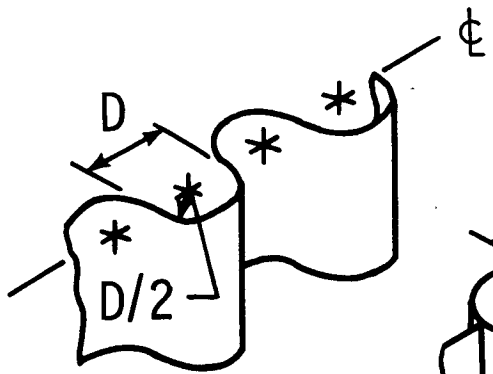

Sine-wave beam (tangent-half circle)

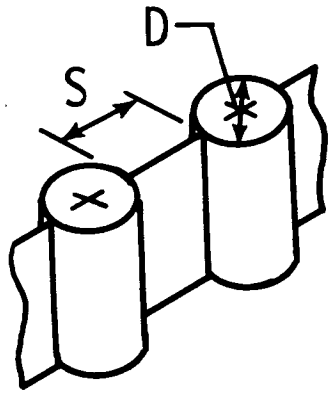

Circular tube stiffened beam

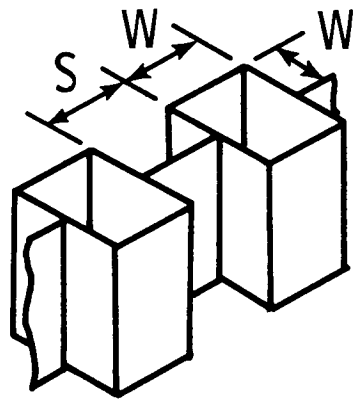

Rectangular tube stiffened beam

Figure 22

ENERGY ABSORPTION OF $\left[\pm 45_S^F /HC\right]_S$ KEVLAR/EPOXY SANDWICH BEAM SPECIMENS

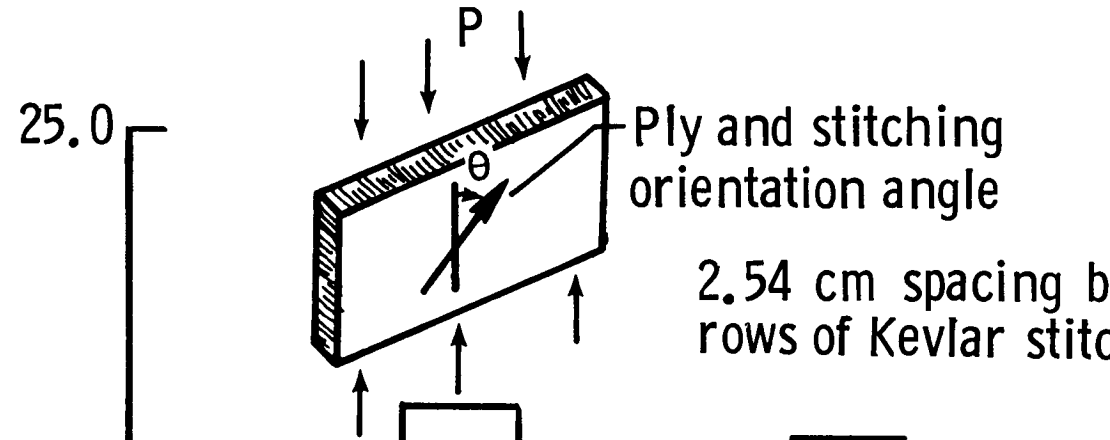

Ply and stitching orientation angle

2.54 cm spacing between rows of Kevlar stitching

Specific sustained crushing stress $\frac{Nm}{g}$

25.0

12.5

0

No stitching

0°

90°

±45°

0°/90°

Kevlar stitching orientation

Figure 23

EFFECTS OF D/t RATIO ON THE ENERGY ABSORPTION OF $[\pm 45]_N$ K/E TUBES AND SINE-WAVE BEAMS

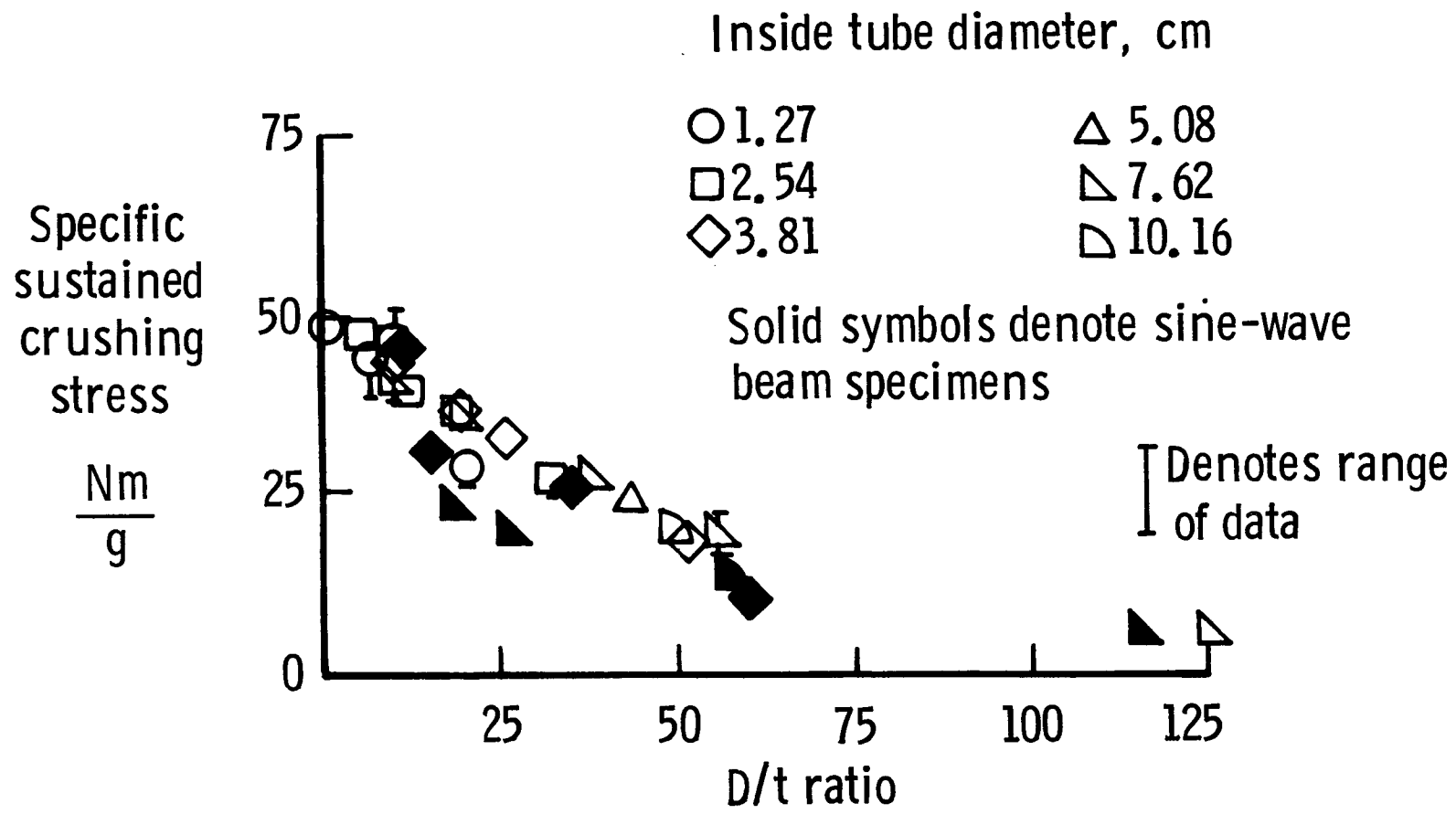

Figure 24

ENERGY ABSORPTION CAPABILITY OF HYBRID COMPOSITE SINE-WAVE BEAMS AND TUBES

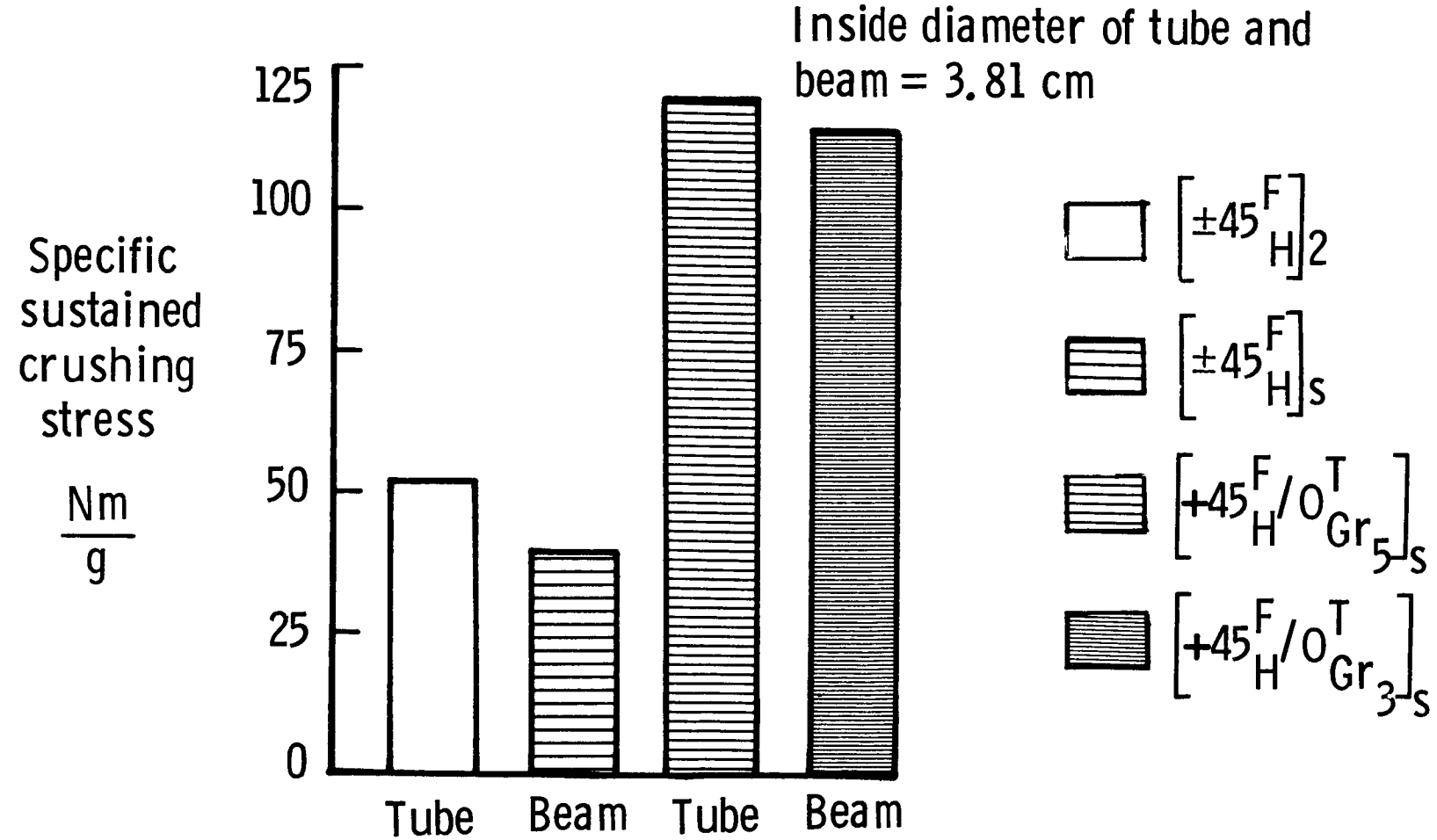

Figure 25

Figure 26

ENERGY ABSORPTION OF CIRCULAR TUBE STIFFENED BEAMS

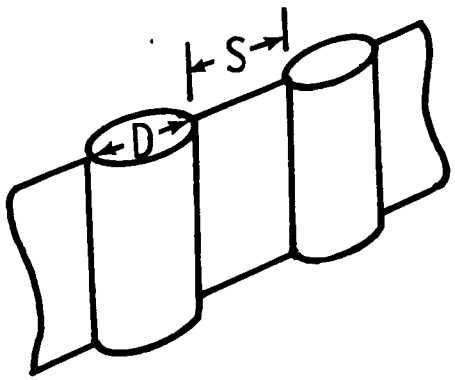

N = Number of stiffeners

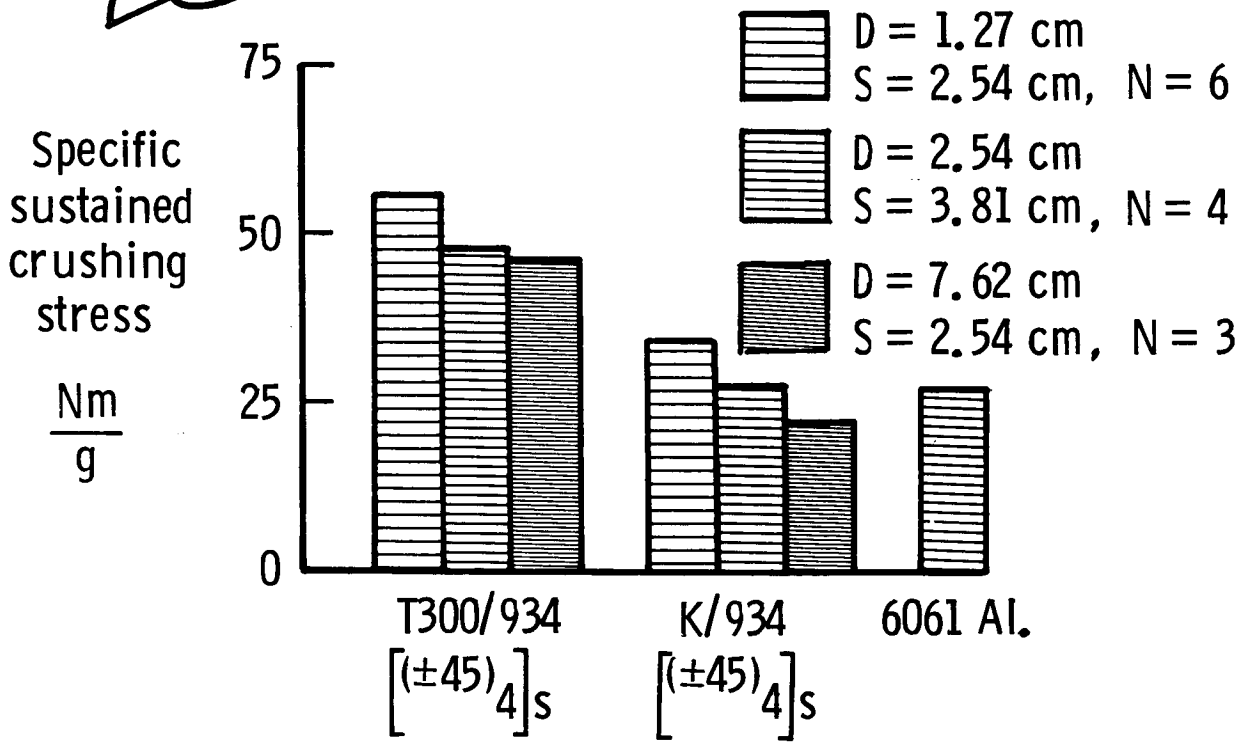

Figure 27

ENERGY ABSORPTION OF RECTANGULAR TUBE STIFFENED BEAMS

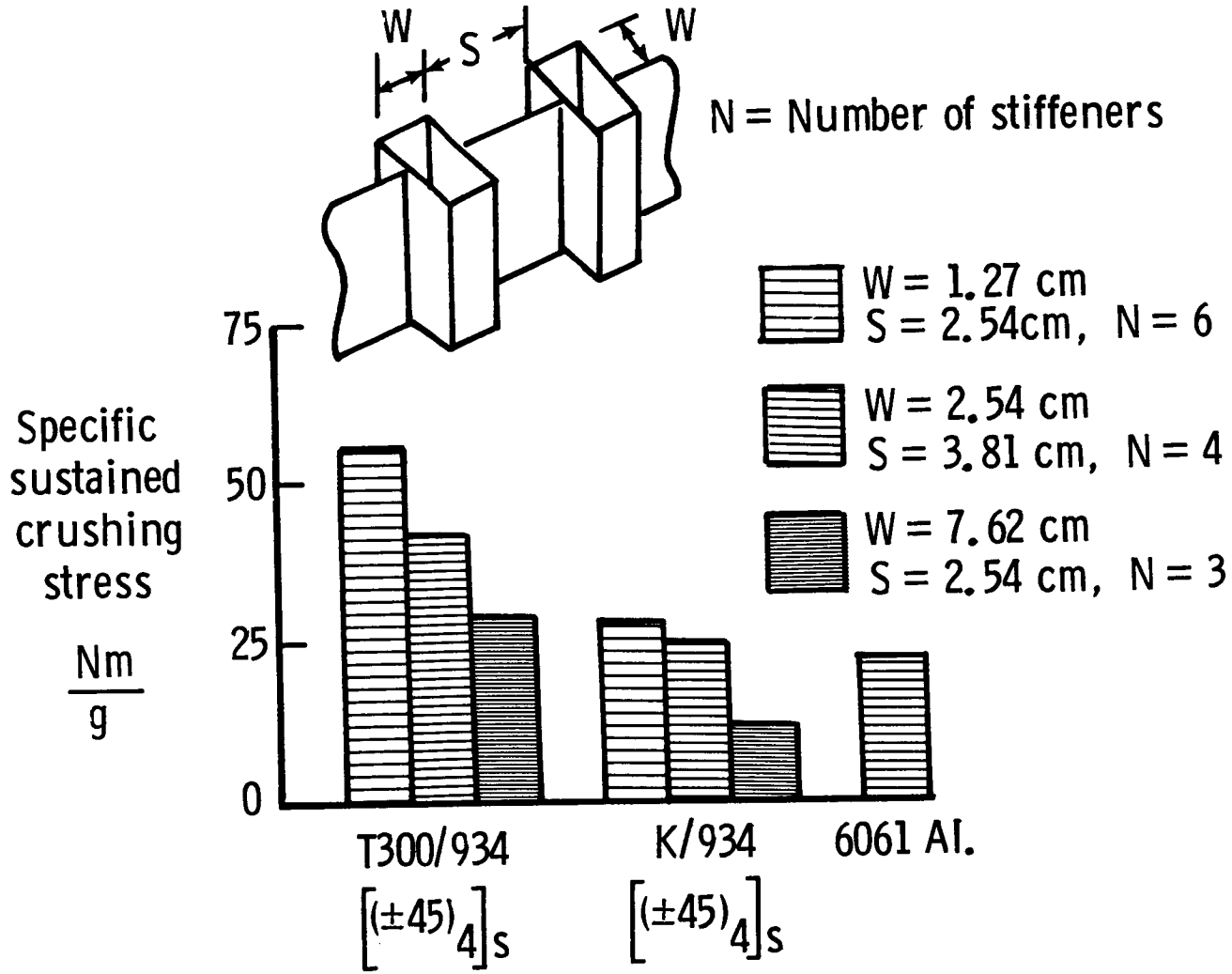

Figure 28

CRUSHED K/934 AND T300/934 $[(\pm 45)_4]_s$ CIRCULAR TUBE STIFFENED BEAMS

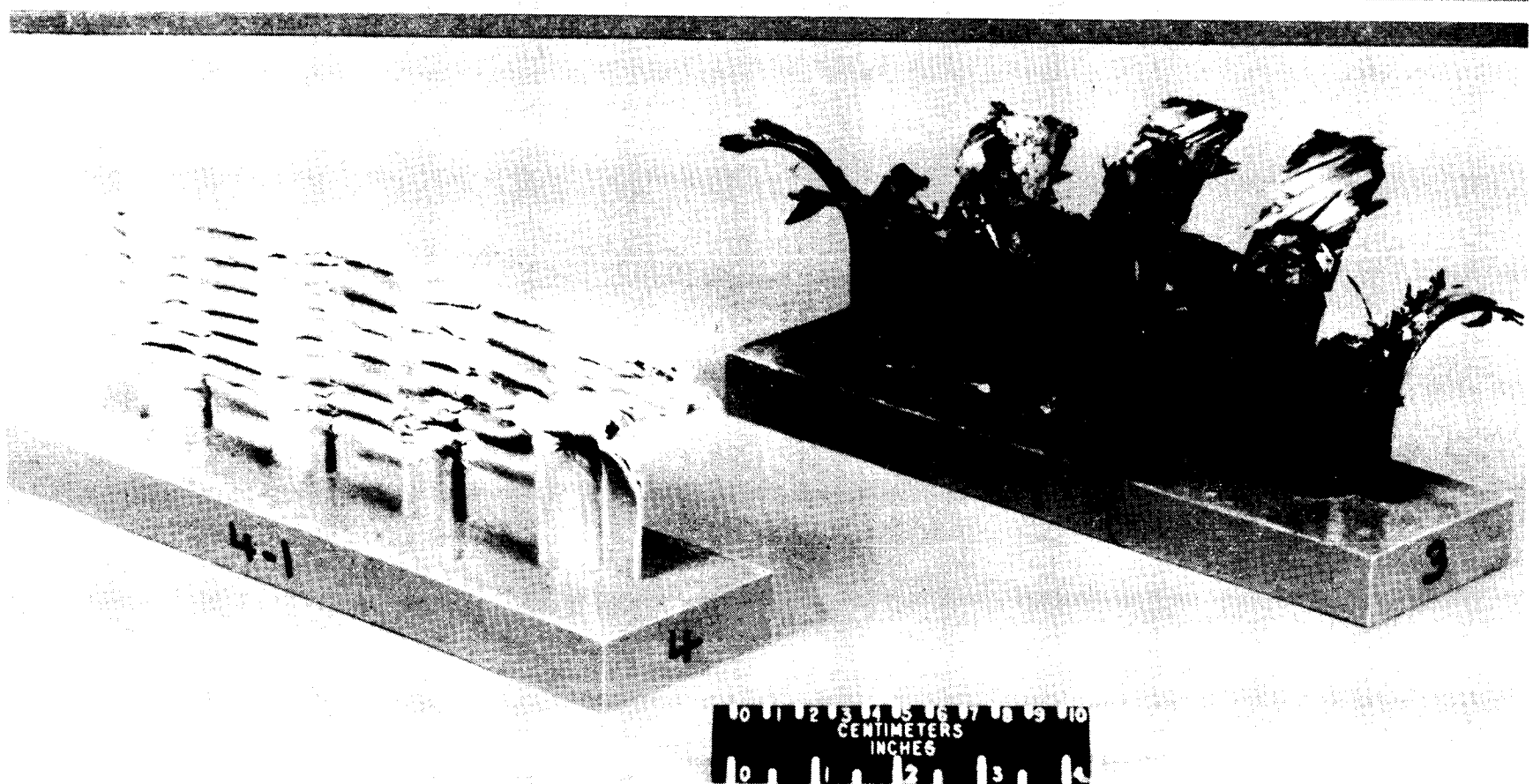

Figure 29

FOUR STIFFENER CIRCULAR CROSS SECTION TUBE STIFFENED BEAM

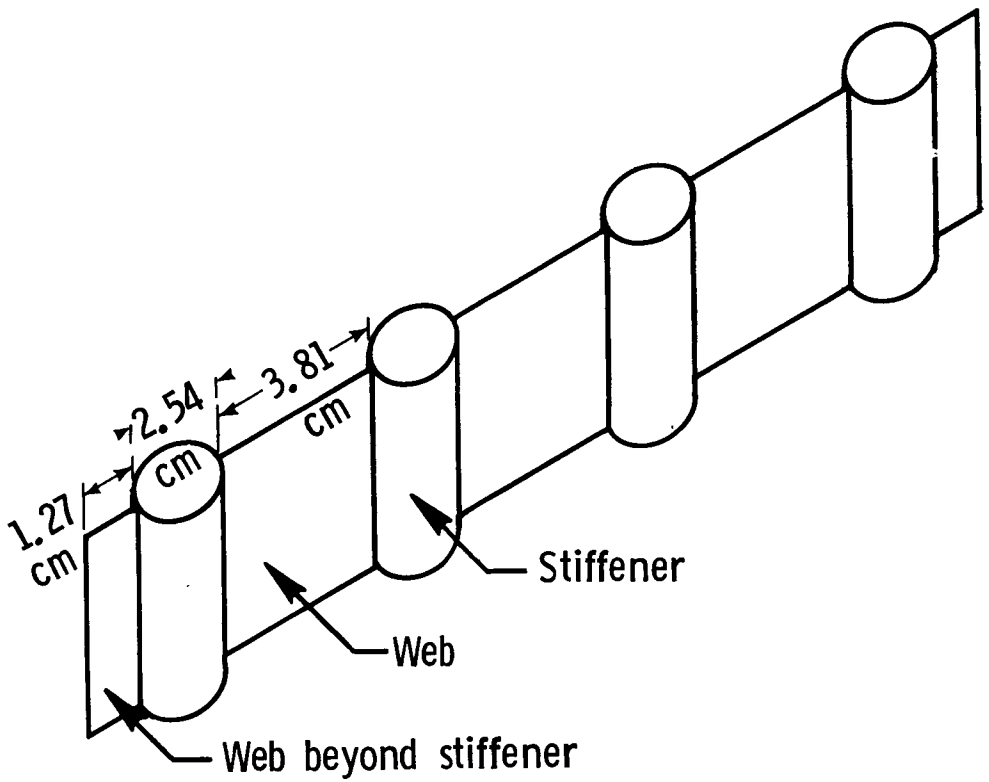

Figure 30

Gr-Ep Frame

GR-EP FRAME CROSS SECTION

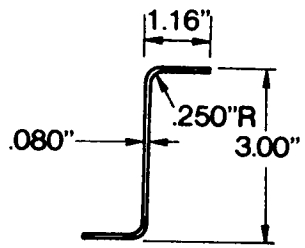

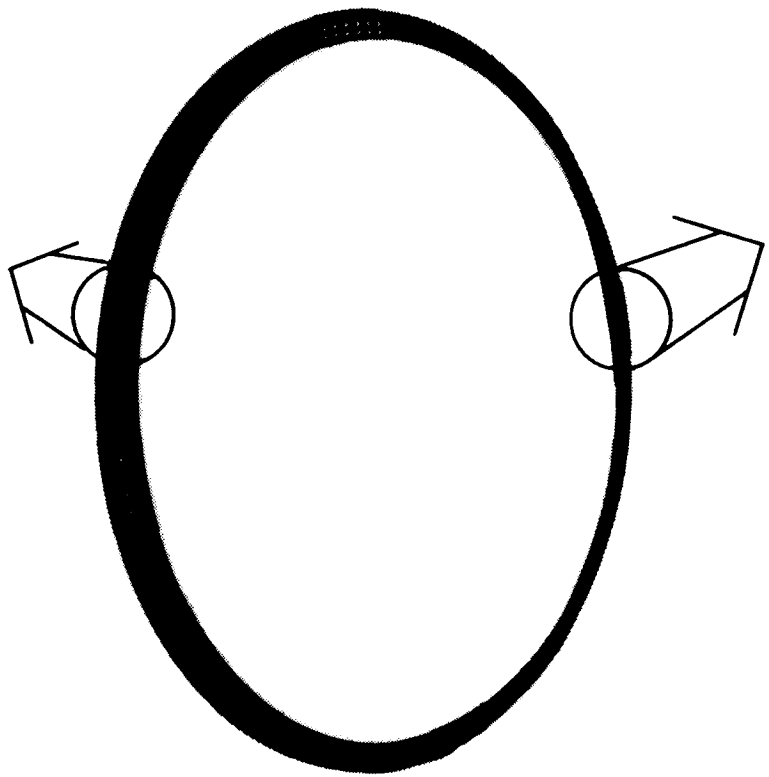

FRAME SPLICE PLATE

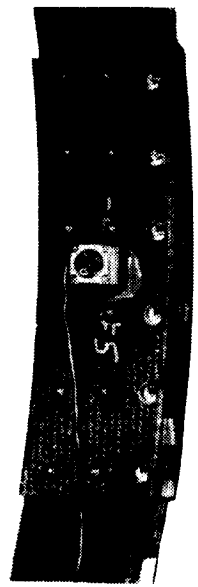

Figure 31

COMPOSITE FRAME STRAIN DISTRIBUTION

TIME = 4.8 MSEC AFTER IMPACT

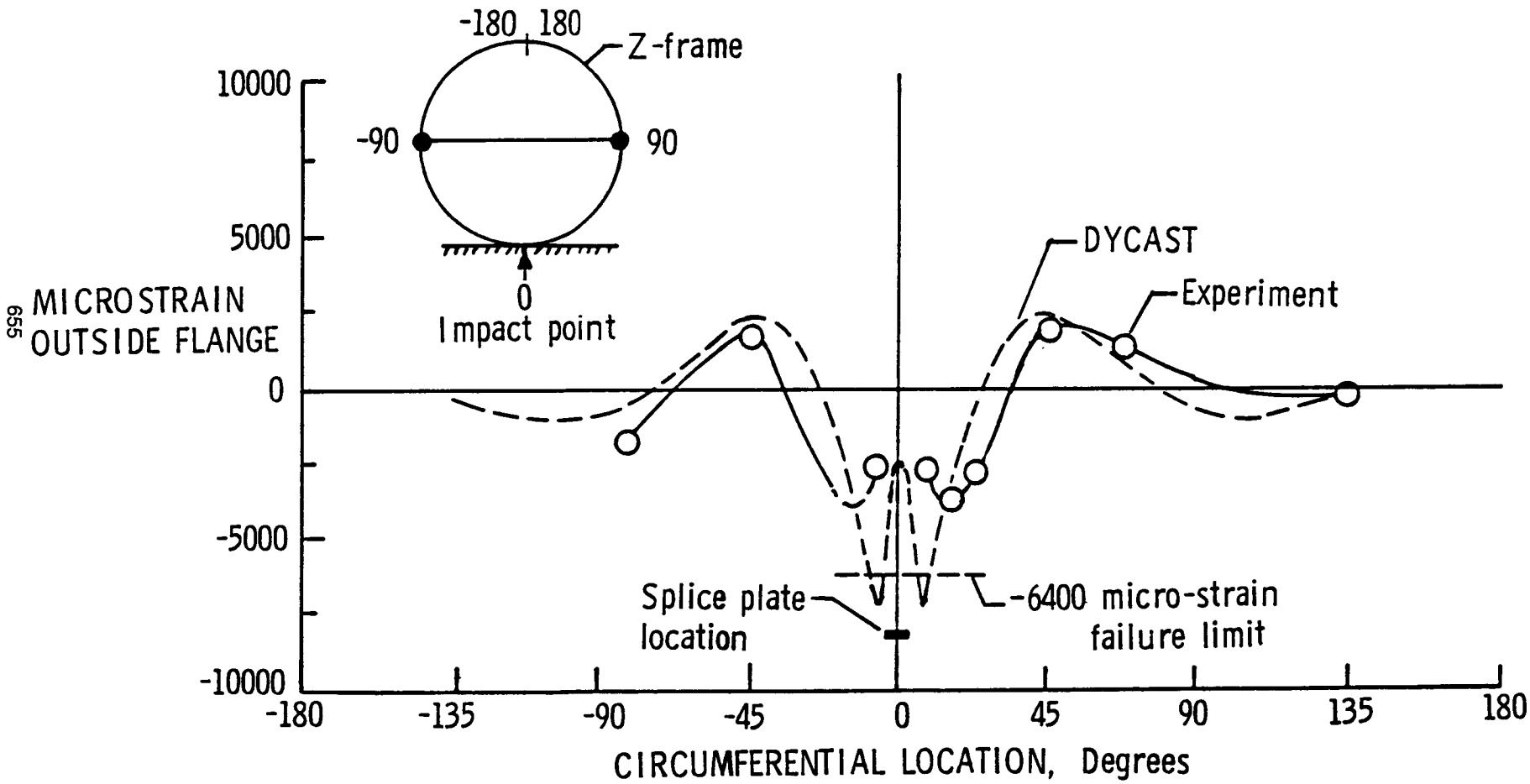

Figure 32